國立臺灣大學工學院化學工程學系

碩士論文

Department of Chemical Engineering

College of Engineering

National Taiwan University

Master Thesis

用於萃取蒸餾塔序列節能技術之比較

Comparison of alternative energy-saving strategies for extractive distillation processes

簡至寬

Chih-Kuan Chien

指導教授：吳哲夫 博士

Advisor: Jeffrey D. Ward, Ph.D.

中華民國 112 年 6 月

June, 2023

doi:10.6342/NTU202301003

國立臺灣大學碩士學位論文
口試委員會審定書

用於萃取蒸餾塔序列節能技術之比較
Comparison of alternative energy-saving strategies for extractive distillation processes

本論文係簡至寬君（R10524137）在國立臺灣大學化學工程研究所完成之碩士學位論文，於民國 112 年 06 月 08 日承下列考試委員審查通過及口試及格，特此證明

口試委員：

J Wang （簽名）
（指導教授）

陳誠亮

錢義隆　李訓業

李奇旺

廖英志

系主任、所長 廖英志（簽名）
（是否須簽章依各院系所規定）

doi:10.6342/NTU202301003

誌謝

隨著北半球日照時間逐漸變長，我也逐漸邁入在程序系統工程實驗室度過的第三個夏天，同時也是最後一個夏天，屬於我的大畢業季終於來到，遙想六年前的一個夏日，對未來感到疑惑與迷茫的我在機緣巧合之下，又或在衝動之下，踏入了化工與材料領域，時光匆匆，歲月悠悠，在這個領域的日子即將告一段落，但我仍然是那個看起來像學弟的簡至寬，且回顧這六年的旅程，一路上不乏幫助我的人，讓我順利地走過這段令人又愛又恨的歲月。

首先，感謝當初不停鞭策我們且把我鞭進台大化工所的張董，某種程度上，因為你的激勵與我才有源源不絕的驅動力，接著必須感謝我的指導教授 Prof. Ward，您就像是一座超大的燈塔兼雷達站，把在由一堆實驗室構成之大海中漂泊的我拉上岸，回憶我們第一次見面的場景，仍然記憶猶新，您充滿活力且直球式的問我要不要加入以及在我表達「要」的瞬間站起拍桌大喊: 「Congratulation！」仍清晰的收錄在我的腦海裡，感謝您在學術與時間上給學生的高度自由以及道地的美式督導風格，不僅協助我讓這份研究順利地發表在 *Separation and Purification Technology*，還讓我度過了一個很有特色的碩士生活，另外也要謝謝 PSE 的其他三位老師在大咪時給予的建議與指導。回憶場景切換到實驗室的日常，感謝偉庭、展生和翌玄三位學長給初來乍到的我許多關照，拉我去打球、吃飯與聊八卦，幫助我熟悉這個生態系，尤其感謝偉庭在研究上經常性的罩我，祝福您在美國的博士生涯也一樣瘋狂。說到博士，免不了的要想到博班學長銘君，感謝您這兩年來不管是在生活上、IT 上還是研究上給的關照，從我進實驗室第一天就開始的各種幫忙與指導，到充滿各種政治不正確或正確的日常閒聊，再到日常的相互提醒下班時間，也感謝聰偉學長時不時的幫忙和分享食物，這些都是我碩士生活的重要元素，謝謝這些沒架子的學長們，當然還有即將跟我一起登出實驗室的三位同學們，謝謝各位這兩年來的關照與日常八卦。最後，大大地感謝我爸媽在生活起居的照料以及經濟上的全力支持，讓我可以無後顧之憂地繼續前進，也感謝我姐不定時的投遞零食、玩物與迷因，謝謝大家的關愛。

碩士生涯已接近尾聲，由衷感謝全部幫助過我的人，希望各位之後的人生都能順順利利，也期許自己在生涯的下一個階段能更加努力，朝目標邁進。

doi:10.6342/NTU202301003

中文摘要

萃取蒸餾為一常見的共沸物分離方法，因其經濟可行性較高且動態控制較為穩定，然而此方法之能耗相當可觀，屬能源密集型單元操作，為此，研究人員發展出數種節能技術以降低其能源消耗，包括熱耦合、液態側流與熱整合等技術。雖然現有文獻不乏大量針對此些技術之研究與應用，但並無快速且通用的標準可幫助程序設計，系統性的評估與篩選方法仍有待發展。

為了解決此不足，本研究藉由十七組二元最小共沸物系統與重夾帶劑配合六種強化蒸餾序列與兩種基本序列之優化結果得出一系列趨勢及現象，且透過觀察與比較這些系統之能耗與年化總成本，本研究提出一個新指標 R_{CB} 用以評估這些節能技術之合適性，針對不同條件與情況快速篩選出較具成本效益之技術和序列。

依照 R_{CB} 之數值變化，本研究歸納出下列結論: (1) 當不考慮再沸器與冷凝器之熱整合時，如 R_{CB} 小於約 8.4，修正型液態側流序列 (MSSS)表現最佳，如 R_{CB} 大於約 8.4，雙塔液態側流序列 (DCSSS)表現最佳。 (2) 當共沸物重成分與夾帶劑之相對揮發度過高時，即使再混合效應相當嚴重，液態側流也不具成本效益。 (3) 當考慮再沸器與冷凝器之熱整合時，如 R_{CB} 小於約 2.2，普通熱整合序列(OSS)具有最佳表現，如 R_{CB} 大於約 2.2，雙塔液態側流熱整合序列(SDCSSS)具有最佳表現。 (4) 當 R_{CB} 較小時，再沸器與冷凝器之熱整合較有效，當 R_{CB} 較大時，液態側流序列較有效。 (5) 當 R_{CB} 介於 2.6 與 8.4 之間時，再沸器與冷凝器之熱整合搭配液態側流序列效果較佳，如 R_{CB} 小於 2.6，液態側流幫助甚微，不建議使用，如 R_{CB} 大於 8.4，再沸器與冷凝器之熱整合幫助甚微，不建議使用。 (6) 當 R_{CB} 較小時，隔牆塔缺乏成本效益，當 R_{CB} 較大時，隔牆塔可降低能耗與成本，但其表現仍不及液態側流序列。

關鍵詞: 萃取蒸餾; 勻相共沸蒸餾; 製程強化; 熱整合; 液態側流; 熱耦合; 隔牆塔; 共沸混合物夾帶劑; 程序優化

doi:10.6342/NTU202301003

ABSTRACT

Extractive distillation is a widely-used but energy-intensive method for separating homogeneous azeotropic mixtures into pure components. The most common case is a minimum-boiling azeotrope separated using a heavy entrainer. Numerous design alternatives have been proposed for reducing energy consumption in such processes, including alternatives with side-streams, column stacking and thermally coupled sequences. However, there is very little guidance in the literature about which alternative is likely to work the best in a given situation.

To address this deficiency, in this work, seventeen industrially-relevant chemical systems comprising two species that form a minimum boiling azeotrope and a heavy entrainer are selected for study. Two ordinary and six energy-saving flowsheet alternatives for extractive distillation processes were also selected. Each of the eight flowsheet alternatives was optimized for each of the 17 chemical systems. A novel metric R_{CB} (the ratio of the entrainer flow rate to the heavy key flow rate) is proposed to facilitate interpretation of the results. The following general trends are observed when comparing flowsheet alternatives for chemical systems with different values of R_{CB}:

(1) When comparing sequences without stacking, the modified side-stream sequence (MSSS) performs better when R_{CB} is smaller (less than about 8.4); the double-column side-stream sequence (DCSSS) performs better when R_{CB} is larger (greater than about 8.4). (2) When the relative volatility of the heavy key and the entrainer is too high, side-stream sequences may be uneconomical even if the

doi:10.6342/NTU202301003

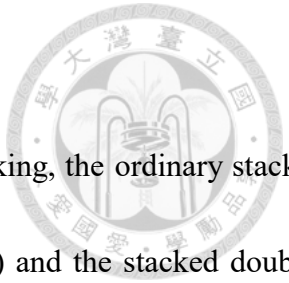

remixing effect is substantial. (3) Considering sequences with column stacking, the ordinary stacked sequence (OSS) performs better when R_{CB} is smaller (less than about 2.2) and the stacked double-column side-stream sequence (SDCSSS) performs better when R_{CB} is larger (greater than about 2.2). (4) Column stacking is more effective when R_{CB} is small, and side streams are more effective when R_{CB} is large. (5) The stacked side-stream sequence is recommended for intermediate values of R_{CB} ($2.6<R_{CB}<8.4$). For $R_{CB}<2.6$, the benefit of the side-stream is minimal and a sequence with stacking only is probably preferred for simplicity. For $R_{CB}>8.4$ the benefit of stacking is minimal and a sequence with a side-stream only is probably preferred for simplicity. (6) The dividing-wall column (DWCU) is not economical when R_{CB} is small and is economical but still less attractive than side-stream sequences when R_{CB} is large.

Keywords: extractive distillation; homogeneous azeotropic distillation; process intensification; heat integration; side stream; thermal coupling; dividing-wall column; column stacking; entrainers; process optimization

doi:10.6342/NTU202301003

CONTENTS

doi:10.6342/NTU202301003

doi:10.6342/NTU202301003

doi:10.6342/NTU202301003

LIST OF FIGURES

doi:10.6342/NTU202301003

doi:10.6342/NTU202301003

doi:10.6342/NTU202301003

doi:10.6342/NTU202301003

LIST OF TABLES

doi:10.6342/NTU202301003

Chapter 1 Introduction

1.1 Overview

Extractive distillation with a heavy entrainer is the most widely-used method for separating volatile liquid mixtures with azeotropes [1]. A disadvantage of extractive distillation is that it is relatively energy intensive [2, 3]. Accordingly, a number of strategies have been applied to reduce the energy consumption of extractive distillation, including liquid side streams [4], thermal coupling [5], and a few heat-integration methods [6].

Liquid side streams can be used to mitigate the so-called the remixing effect [7]. The side stream removes a liquid mixture rich in component B (the heavy key) from the extractive column and routes it to a stage in the entrainer recovery column where the composition is close to that of the side stream, as shown in Figure 1.

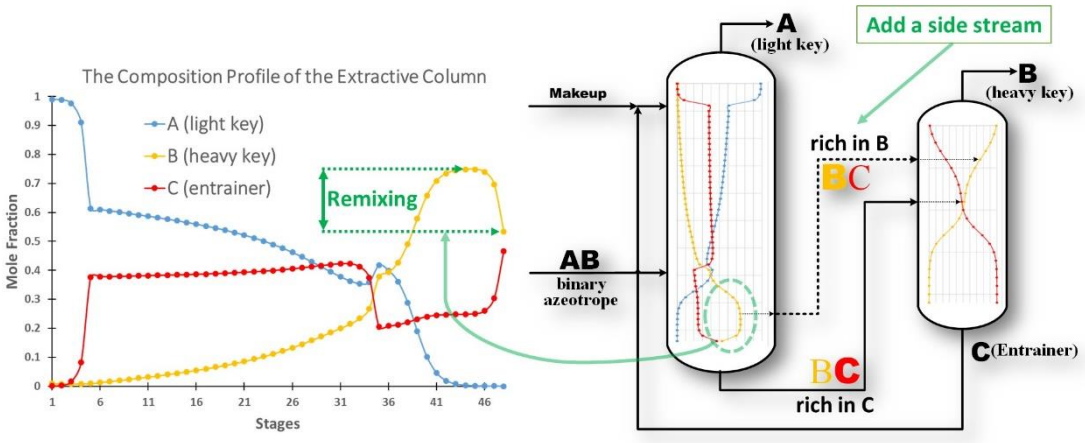

Figure 1. The remixing effect in the conventional sequence and the purpose of adding a side stream

The side stream reduces remixing in the bottom of the extractive column, which can

doi:10.6342/NTU202301003

reduce the energy demand in the recovery column.

Thermal coupling can be achieved by removing a condenser or a reboiler of a distillation column and replacing it with vapor and liquid interconnections. When all sections of a thermally coupled distillation sequence are combined in a single shell, the result is called a dividing-wall column (DWC) [8], as shown in Figure 2.

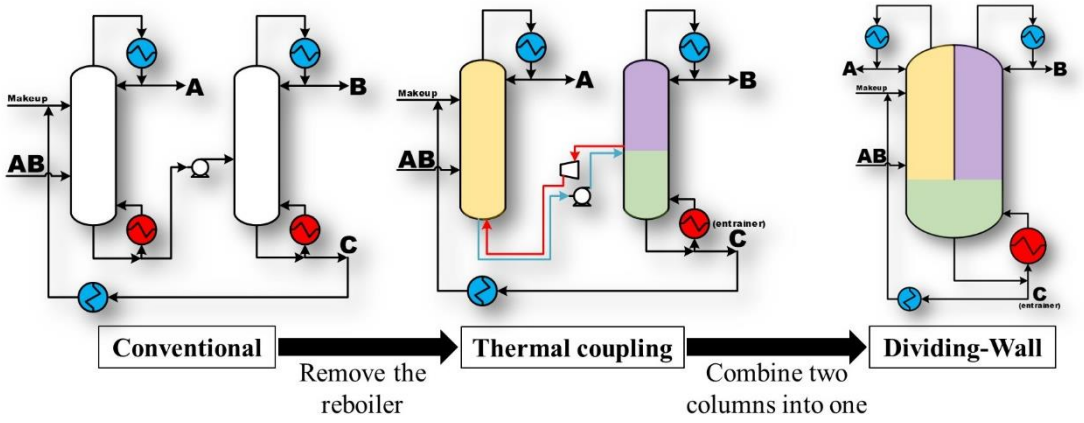

Figure 2. The concept of thermal coupling and the dividing-wall column

Heat-integrated distillation sequences incorporate one or more strategies for heat integration including intermediate heating, preheating, column stacking, and vapor recompression heat pumps, as illustrated in Figure 3. Intermediate heating refers to the strategy of using a side reboiler attached to the recovery column to recover some of the sensible heat of the heavy entrainer [9]. Preheating recovers sensible heat from the heavy entrainer recycle stream to heat the feed stream [10]. Vapor recompression heat pumps compress the top vapor stream of a distillation column to a higher pressure so that it condenses at a higher temperature, becoming a heat source providing latent heat to a

doi:10.6342/NTU202301003

reboiler [11, 12]. Column stacking refers to using the top vapor stream of one column to power the reboiler of another column by adjusting the operating pressure to meet a desired temperature driving force for heat transfer [13, 14].

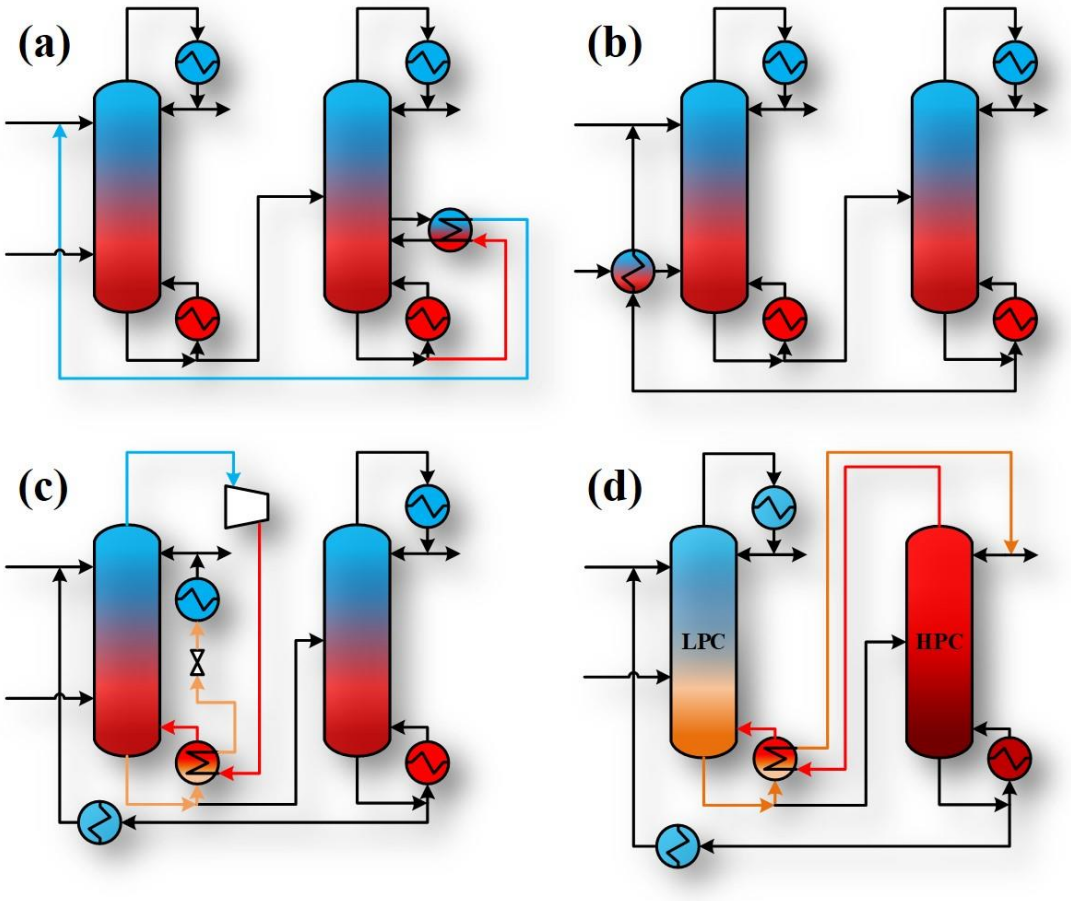

Figure 3. Several heat integration strategies: (a) intermediate heating, (b) preheating, (c) vapor recompression heat pumps, (d) column stacking

1.2 Literature Survey

Researchers have studied the above-mentioned strategies individually or compared them for a single separation task over the years. Hernandez [15] found that thermally coupled sequences could reduce energy consumption by 30% in a bioethanol purification

doi:10.6342/NTU202301003

process. Errico et al. [16] found that dividing-wall columns could decrease the cost of bioethanol production. Cui et al. [17] proposed a systematic method to synthesize distillation sequences and showed that thermally coupled sequences could reduce energy consumption by more than 30% compared to the base case. Zhang et al. [18] and Shi et al. [19] studied the same side-stream sequence with feed preheating, and showed that it reduced energy consumption by more than 10%. Luyben [20] studied the separation of acetone and methanol. He compared the performance of pressure-swing distillation and extractive distillation and found that extractive distillation with column stacking heat integration was preferable. Tututi-Avila et al. [21] investigated side streams, thermal coupling and column stacking. They showed that these strategies were effective for conserving energy, especially the combination of a side stream and column stacking. Zhang et al. [22] simulated the separation of isopropyl alcohol/diisopropyl ether with three different entrainers and compared the thermally coupled sequence and the side-stream sequence. They found that the thermally coupled sequence performed better than the side-stream sequence. Xu et al. [23] applied heat pumps, preheating, and column stacking to a process for wastewater treatment. The combination improved energy efficiency and reduced CO_2 emissions substantially. Yang et al. [24] studied heat pump-assisted side-stream columns with multi-objective optimization and obtained significant improvements in thermodynamic efficiency, CO_2 emissions, and costs. In summary,

doi:10.6342/NTU202301003

researchers have investigated energy conservation strategies extensively and suggested criteria for assessing whether they are likely to be suitable for a particular situation based on metrics such as the coefficient of performance (COP) for heat pumps [25] and the ratio of the entrainer flow rate (ROE) at different pressures for determining the operating pressure of the extractive column in an extractive distillation sequence [26]. Anokhina and Timoshenko [27], studied partially thermally coupled extractive distillation systems (PCEDS) and compared them with the conventional sequences for a substantial number of mixtures. The suggested the heuristic that PCEDS is likely to save energy if the reflux ratio of the entrainer recovery column is greater than 1.

1.3 Problem Statements

Although researchers have applied various energy-saving strategies to different extractive distillation processes, there has been little systematic comparison of the results and little general guidance about which strategy is likely to work best in a given situation. Therefore, in this work, a large set of data was collected by optimizing each of eight different flowsheet alternatives for each of 17 industrially-relevant azeotropic mixtures with heavy entrainers. This represents a very substantial amount of engineering effort, as candidate azeotropic systems had to be identified, a thermodynamic model validated, and eight flowsheet alternatives optimized for each of the 17 azeotropic systems.

The results for each of the 17 azeotropic systems are interesting in their own right

doi:10.6342/NTU202301003

and can provide guidance about reducing energy consumption in the separation of each individual mixture. More importantly, however, when the data are compared across mixtures, general trends emerge about which energy-saving strategies work best in a given situation. In particular, a novel index R_{CB} (the ratio of the entrainer flow rate to the flow rate of the heavy key) is proposed in this work. It is shown for the extractive distillation processes studied in this work that the relative attractiveness of energy saving strategies can be understood in terms of the value of R_{CB}.

1.4 Thesis Organization

The structure of this dissertation is arranged as follows: The definition of R_{CB}, the extractive distillation sequences considered in this study, seventeen binary minimum boiling azeotropes chosen, the methods for modelling distillation sequences, and the algorithm for process optimization are introduced in Chapter 2. The meanings of R_{CB} are discussed in Chapter 3, and the optimization results are shown in Chapter 4. The conclusions drawn from the results are given in Chapter 5. Optimization variables for each extractive distillation sequence are demonstrated in Appendix A. Binary interaction parameters for each case are listed in Appendix B. The flowchart for calculating parameters for the simulated annealing algorithm is provided in Appendix C. Information about cost calculations is given in Appendix D.

doi:10.6342/NTU202301003

Chapter 2 Methods

In this part of the thesis, the definition of R_{CB} is given in Section 2.1. Extractive distillation sequences, azeotropes, and entrainers are shown in Section 2.2 and 2.3. The methods for process simulation and optimization are presented in Section 2.4 and 2.5.

2.1 The Definition of R_{CB}

For a minimum boiling azeotrope with a heavy entrainer, the conventional extractive distillation sequence includes two columns, the extractive column (the 1st column) and the recovery column (the 2nd column), as shown in Figure 4. The entrainer flows into the 1st column at the top of the extractive section and mixes with the fresh AB mixture fed at the bottom of the extractive section, breaking the azeotrope.

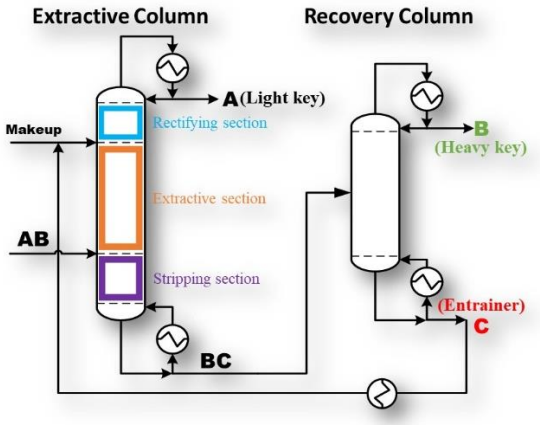

Figure 4. The conventional sequence for extractive distillation with a heavy entrainer

The index R_{CB} proposed in this work is defined as the ratio of the flow rate of stream C to stream B:

$$R_{CB} = \frac{C}{B} \quad (1)$$

doi:10.6342/NTU202301003

where C and B denote the molar flow rate of stream C (entrainer) and stream B (heavy key), respectively, after optimization of the conventional sequence. As will be shown, general trends in the data for the performance of energy-saving strategies can be stated in terms of R_{CB}. R_{CB} should not be confused with R_{EF}, the entrainer to feed ratio [28], which is used to quantify the effectiveness of an entrainer. Interpretations of R_{CB} are presented in Chapter 3.

2.2 Extractive Distillation Sequences

The energy-intensified sequences considered in this work are shown in Figure 5. The conventional sequence (CS) is taken to be the base case for each azeotrope. If the fresh feed is not close to the azeotropic composition, a pre-concentrator is considered to determine whether it can reduce cost, as shown in Figure 5(b). The dividing-wall column with an upper partition (DWCU) [29] is shown in Figure 5(c). In the process simulator, DWCU is represented with the thermodynamically equivalent flowsheet shown in Figure 6 because DWCs are not natively supported in the simulator. Figures 5(d) and 5(e) show two liquid-side-stream sequences [4, 30] that are often studied because they are especially effective at mitigating the remixing effect. Figures 5(f), 5(g), and 5(h) are sequences that use column stacking [21, 31], a commonly-used method for heat integration. The optimization variables for these sequences are provided in Appendix A. Red dashed arrows in flowsheets indicates the heat exchange between condenser and reboiler, as

doi:10.6342/NTU202301003

shown in Figure 7.

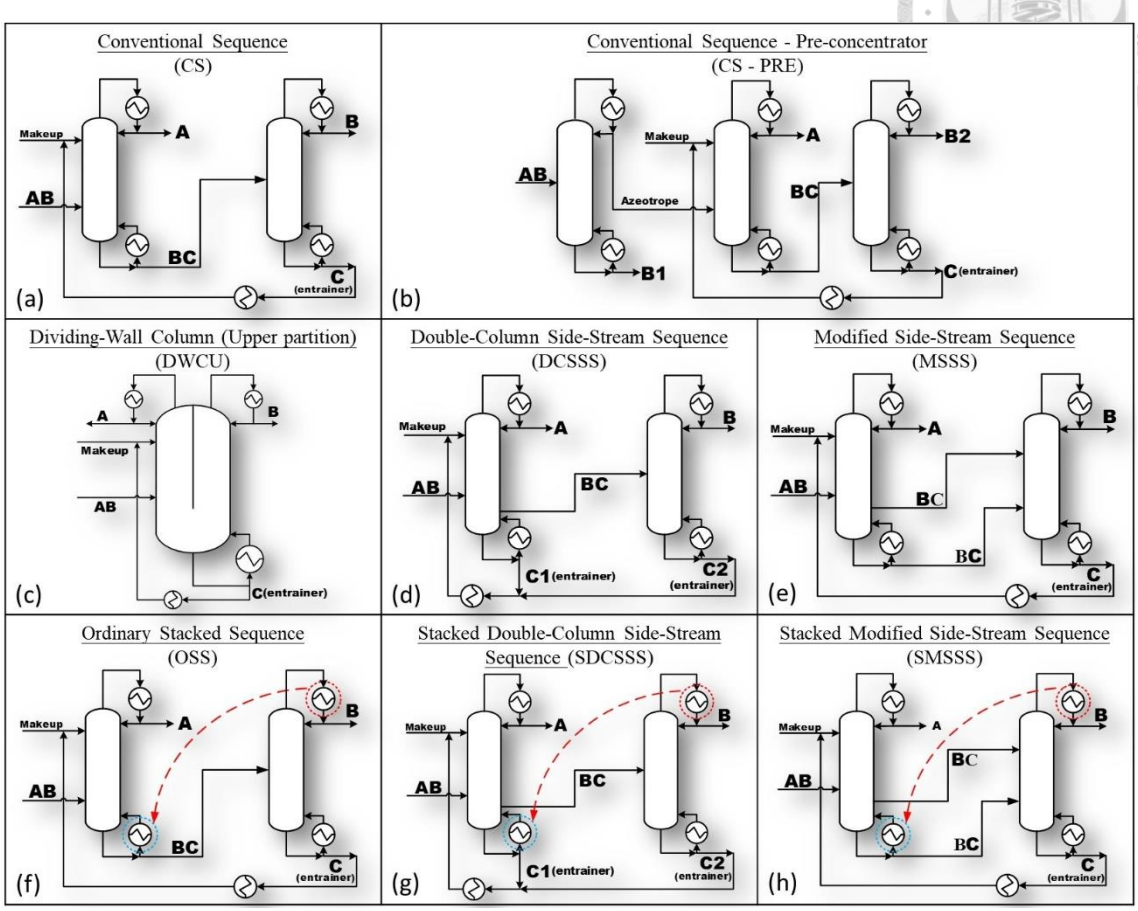

Figure 5. The extractive distillation sequences considered in this work: (a) the conventional sequence, (b) the conventional sequence with a pre-concentrator, (c) the dividing-wall column with an upper partition, (d) the double-column side-stream sequence, (e) the modified side-stream sequence, (f) the ordinary stacked sequence, (g) the stacked double-column side-stream sequence, and (h) the stacked modified side-stream sequence

doi:10.6342/NTU202301003

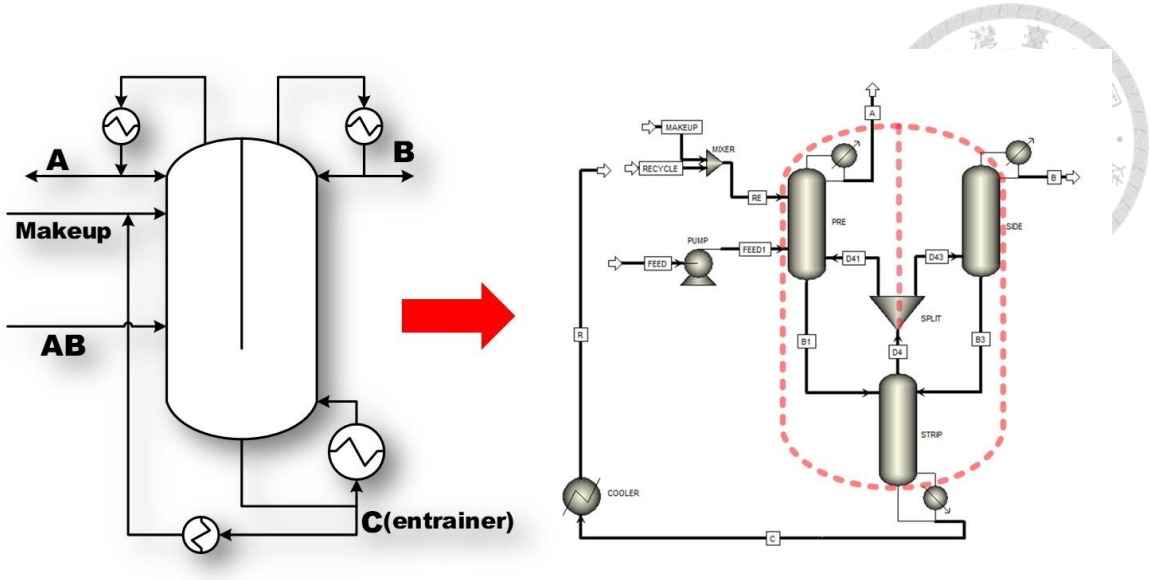

Figure 6. Implementation of DWCU in Aspen Plus

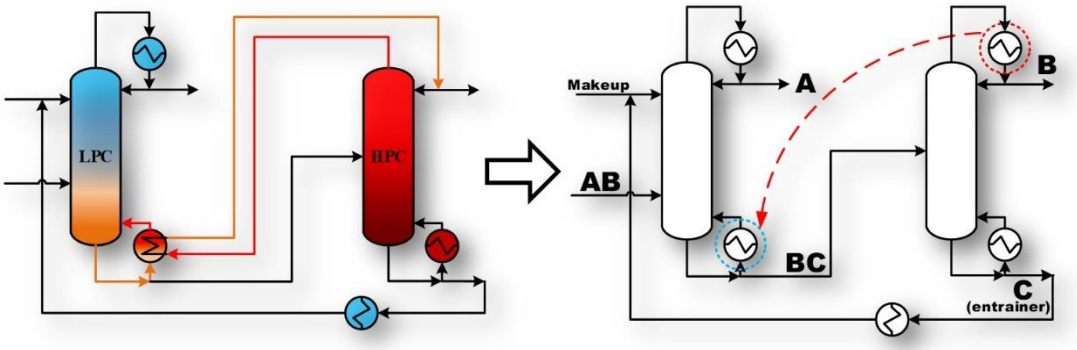

Figure 7. A simplified flowsheet for a stacked sequence

2.3 Azeotropes and Entrainers

The 17 azeotropic systems selected from the literature for this study are shown in Table 1. These cases were selected primarily for two reasons. One is that column stacking is feasible (there is a moderate temperature difference between the boiling points of B & C), for example, cases No. 1-7, 9, 10, 12-14. The other reason is in order to ensure a wide range of values of R_{CB}, such as cases No. 8, 11, 15-17. For azeotropes commonly studied in the past, such as methanol/dimethyl carbonate, diisopropyl ether/isopropyl alcohol, and

doi:10.6342/NTU202301003

acetone/methanol, both equimolar and azeotropic feed compositions are considered in this work. The feed quality of every case is set at saturated liquid and the recovery of sensible heat by heat exchange with the feed is not considered. The feed rate is set to be 100 kmol/hr in cases 1–15 and 200 kmol/hr in cases 16 and 17. Table 2 shows the thermodynamic models and the literature references for each case. The binary interaction parameters are given in Appendix B.

doi:10.6342/NTU202301003

Table 1. The azeotropic mixtures studied in this work

Case No.	Components		Boiling Point (B.P.)		Azeotrope (at 1 atm)		C (Entrainer)	C B.P.	Fresh Feed (mole)
	A (light key)	B (heavy key)	A	B	A/B (mole)	B.P.			
1	Methanol	Toluene	64.7°C	110.6°C	0.887/0.113	63.5°C	Butyl butanoate	165.0°C	0.5/0.5
2	Methanol	Toluene	64.8°C	110.6°C	0.887/0.113	63.5°C	Butyl propanoate	145.1°C	0.5/0.5
3	Methanol	Dimethyl carbonate	64.7°C	90.3°C	0.8533/0.1467	63.8°C	4-methyl-2-pentanone	116.0°C	0.5/0.5
4	Methyl tert-butyl ether	Ethanol	55.1°C	78.3°C	0.93/0.07	55.0°C	Butanol	118.8°C	0.5/0.5
5	Acetone	Heptane	56.1°C	98.4°C	0.925/0.075	55.9°C	Butyl propanoate	145.1°C	0.5/0.5
6	Diisopropyl ether	Isopropyl alcohol	68.3°C	82.2°C	0.77/0.23	66.2°C	Methoxyethanol	124.5°C	0.5/0.5
7	Methanol	Vinyl acetate	64.7°C	72.5°C	0.59/0.41	58.9°C	Allyl acetate	104.0°C	0.5/0.5
8	Ethanol	Cyclohexane	78.3°C	80.7°C	0.44/0.56	64.8°C	Butyl propanoate	145.1°C	0.4/0.6
9	Methanol	Dimethyl carbonate	64.7°C	90.3°C	0.8533/0.1467	63.8°C	4-methyl-2-pentanone	116.0°C	0.8533/0.1467
10	Acetone	Methanol	56.1°C	64.7°C	0.775/0.225	55.7°C	Water	100.0°C	0.5/0.5
11	Benzene	Acetonitrile	80.1°C	81.7°C	0.52/0.47	73.0°C	Dimethyl sulfoxide	190.9°C	0.5/0.5
12	Diisopropyl ether	Isopropyl alcohol	68.3°C	82.2°C	0.77/0.23	66.2°C	Methoxyethanol	124.5°C	0.75/0.25
13	Acetone	Methanol	56.1°C	64.7°C	0.775/0.225	55.7°C	Water	100.0°C	0.77/0.23
14	Ethyl acetate	Heptane	77.1°C	98.4°C	0.87/0.13	76.9°C	Xylene	138.4°C	0.85/0.15
15	Chloroform	Methanol	61.2°C	64.7°C	0.65/0.35	53.4°C	Propanol	97.2°C	0.5/0.5
16	Ethanol	Water	78.3°C	100°C	0.89/0.11	78.2°C	Ethylene glycol	197.2°C	0.88/0.12
17	Ethanol	Water	78.3°C	100°C	0.89/0.11	78.2°C	Ethylene glycol/Glycerol (0.6/0.4)	197.2°C/287.9°C	0.88/0.12

doi:10.6342/NTU202301003

Table 2. The thermodynamic model and references for each case

Case No.	Model	References
1	NRTL	He et al. 2021 [32]
2	NRTL	He et al. 2021 [32]
3	NRTL	Matsuda et al. 2011 [33], Hu & Cheng 2017 [34]
4	NRTL	Arce et al. 1999 [35]
5	UNIQUAC	Zhang et al. 2021 [36]
6	NRTL	Lladosa et al. 2007 [37], Luo et al. 2014 [38], Zhang et al. 2020 [22]
7	NRTL	Resa et al. 2002 [39]
8	NRTL	Zhang et al. 2020 [40]
9	NRTL	Matsuda et al. 2011 [33], Hu & Cheng 2017 [34]
10	UNIQUAC	Luyben 2008 [41], Wang et al. 2020 [42]
11	WILSON	Yang et al. 2013 [43]
12	NRTL	Lladosa et al. 2007 [37], Luo et al. 2014 [38], Zhang et al. 2020 [22]
13	NRTL	Luyben 2008 [41], Wang et al. 2020 [42]
14	WILSON	Díaz & Tojo 2002 [44], Liu et al. 2020 [45]
15	NRTL	Hosgor et al. 2014 [46], Cao et al. 2017 [47]
16	NRTL	Ravagnani et al. 2010 [48]
17	NRTL	Gil et al. 2014 [49], Jaime et al. 2018 [50]

2.4 Process Optimization

In this work, all processes are simulated using Aspen Plus. A simulated annealing (SA) algorithm is used to optimize the flowsheets [51]. The SA algorithm is written in MATLAB and connected to Aspen Plus via the automation server.

Simulated annealing is a stochastic algorithm in which a change in the energy state may occur in one of two ways. One is accepting the new energy state unconditionally, and the other is accepting a new energy state conditionally. Unconditional acceptance occurs when the new energy state is lower than the lowest energy state found since the

doi:10.6342/NTU202301003

procedure started. Conditional acceptance refers to accepting the new energy state that is larger than the previous one. This happens based on the following criteria:

$$P_{\text{accept}} = \frac{P_{\text{E-NEW}}}{P_{\text{E-OLD}}} = \exp\left(\frac{E_{\text{NEW}} - E_{\text{OLD}}}{T}\right) \quad (2)$$

where E_{NEW} and E_{OLD}, and T represent the new energy state, the old energy state, and annealing temperature, respectively. The acceptance of larger energy states can surmount a barrier during optimization, escaping from the local minimum, as shown in Figure 8.

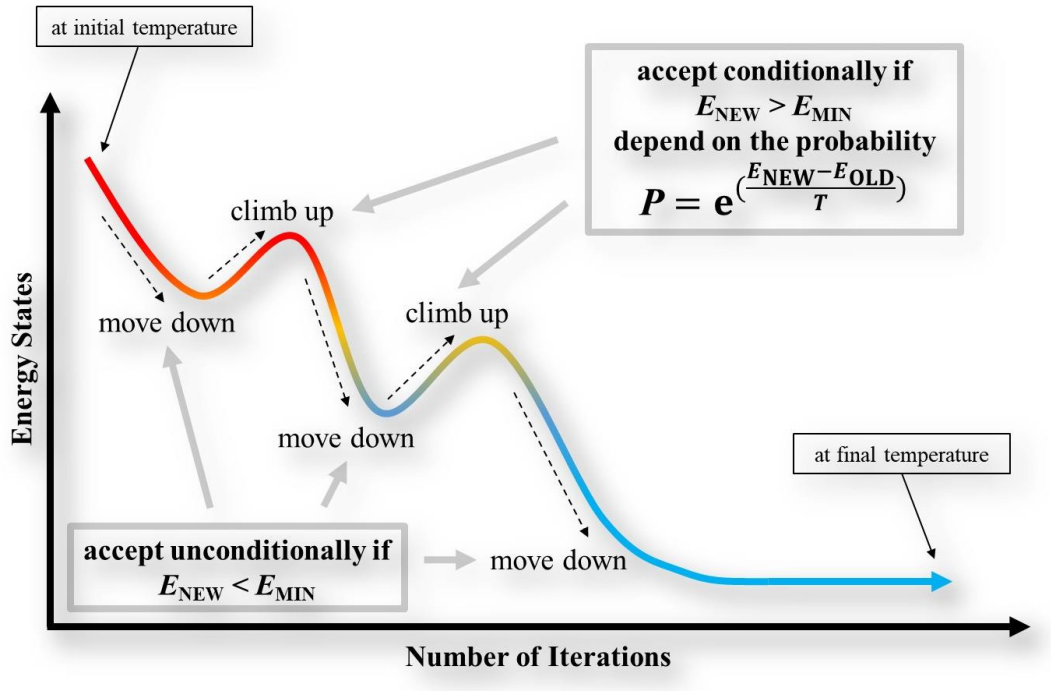

Figure 8. The concept of the simulated annealing algorithm

The objective function for optimization is the total annual cost (TAC) [52, 53] with a payback period of three years, as shown below:

$$\text{TAC} = \text{Operating Cost (OC)} + \frac{\text{Capital Cost (CC)}}{3\ \text{(Payback Period)}} \quad (3)$$

The capital costs include the column shell, reboilers, condensers, heat exchangers, pumps, and vacuum equipment. The operating costs include hot utilities, cold utilities,

doi:10.6342/NTU202301003

and electricity. The pressure drop across each theoretical stage is taken to be 0.0068 atm. The column diameter is calculated using the built-in tray sizing feature in Aspen Plus. Details about the cost calculations are given in Appendix D. Since the objective function is TAC, the energy states in the SA algorithm are replaced with TAC. A flowchart for the SA algorithm with TAC as the objective function is shown in Figure 9, and a flowchart for calculating parameters for the SA algorithm can be found in Appendix C.

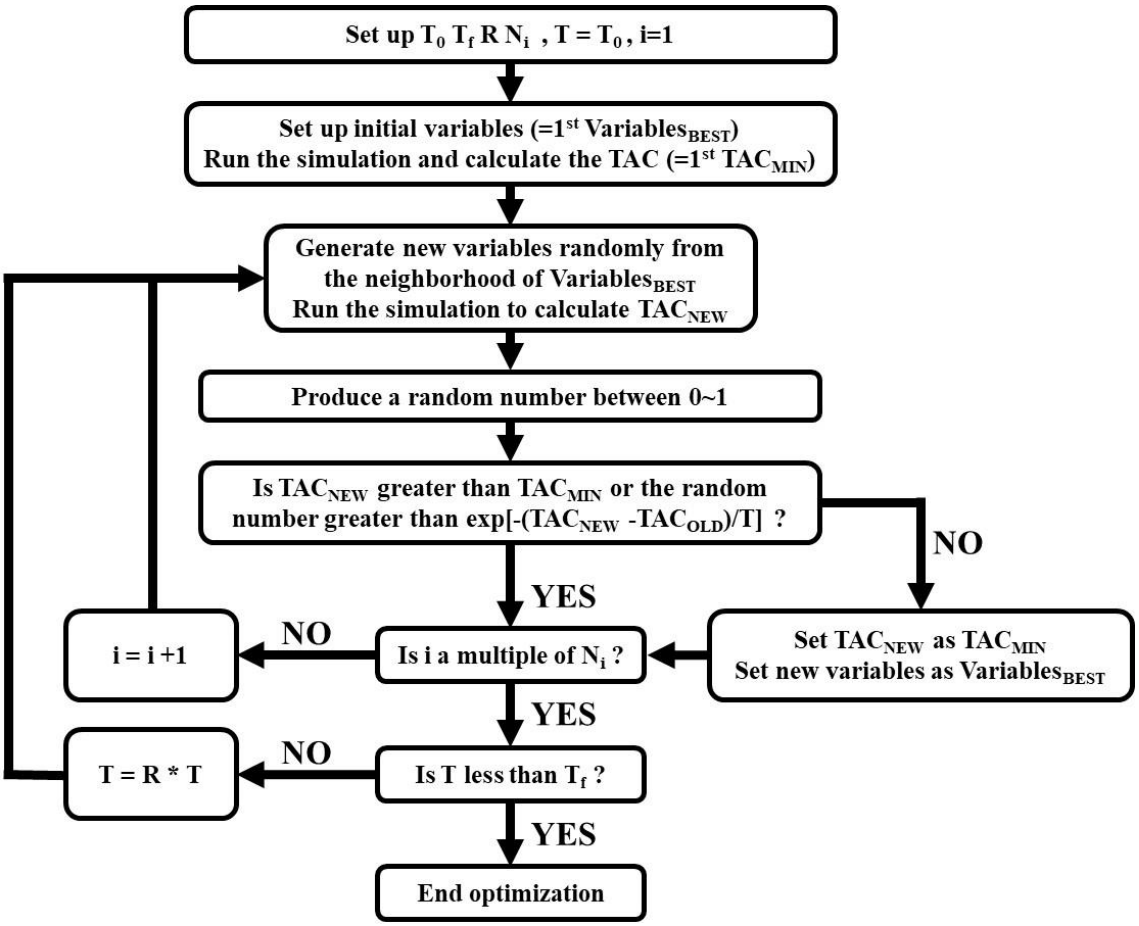

Figure 9. The flowchart for the simulated annealing algorithm

doi:10.6342/NTU202301003

2.5 Initial Guesses & Results Validation

The algorithm for optimization throughout this study is the Simulated Annealing, with a two-phase optimization approach conducted to find out better initial guesses and verify the correctness of the results. The first phase identifies multiple local minima using different variable values that are difficult to determine initially (such as the entrainer flow rate, side stream flow rate of the MSSS, and vapor split ratio of the DWCU). The second phase takes the variables of these local minima as starting points for further optimization to obtain the final results. For instance, in the conventional sequence for Case No. 5, the design variables include the number of stages, feed stage, entrainer feed stage, column pressure, and entrainer flow rate. To ensure the duty and the reflux ratio fall within a reasonable range, a larger initial value for the number of stages is typically used. This can be easily determined by checking the output (the reflux ratio and duty) in Aspen Plus while building the process model, as shown in Figure 10.

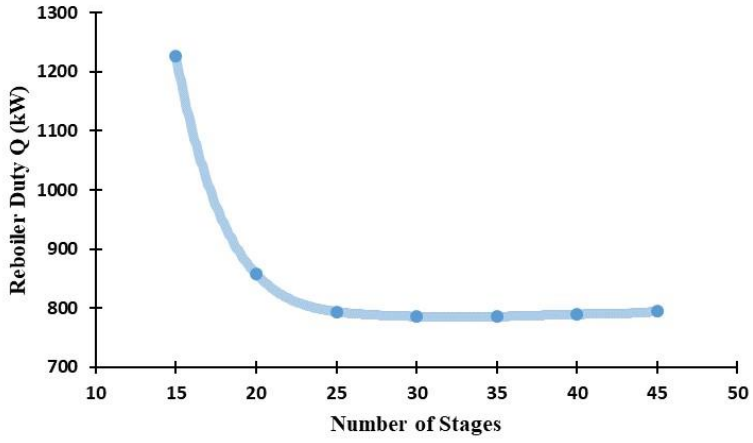

Figure 10. The number of stages of a distillation versus the reboiler duty with all other variables fixed (Case No.5, the 2nd column)

doi:10.6342/NTU202301003

In extractive distillation sequences with a heavy entrainer, the entrainer feed stage should be located at the upper part of the column, while the fresh feed stage should be at the lower part [54]. The number of theoretical stages in each section (extractive, rectifying, and stripping) of the extractive column can be verified by crosschecking the results. It is important to confirm that the differences in the number of stages for each section between alternatives are insignificant or justifiable, as demonstrated in Figure 11 and Table 3. In this case, each sequence has the same size of the rectifying section. The optimized DWCU has a smaller extractive section than the others since its optimum entrainer flow rate is larger than the other sequences, which makes sense. The stripping sections of DWCU and DCSSS are larger than the other two because the former recovers all entrainer with only one column and the latter recovers some entrainer at the bottom of the extractive column, requiring a larger stripping section naturally and inevitably.

Table 3. The size of each section in the extractive column after optimization

Sequence	Number of Stages (NS)			Entrainer flow rate (kmol/hr)
	NS of the rectifying section	NS of the extractive section	NS of the stripping section	
CS	3	27	4	44.5
MSSS	3	25	6	46.6
DCSSS	3	26	13	45
DWCU	3	19	14	50.8

doi:10.6342/NTU202301003

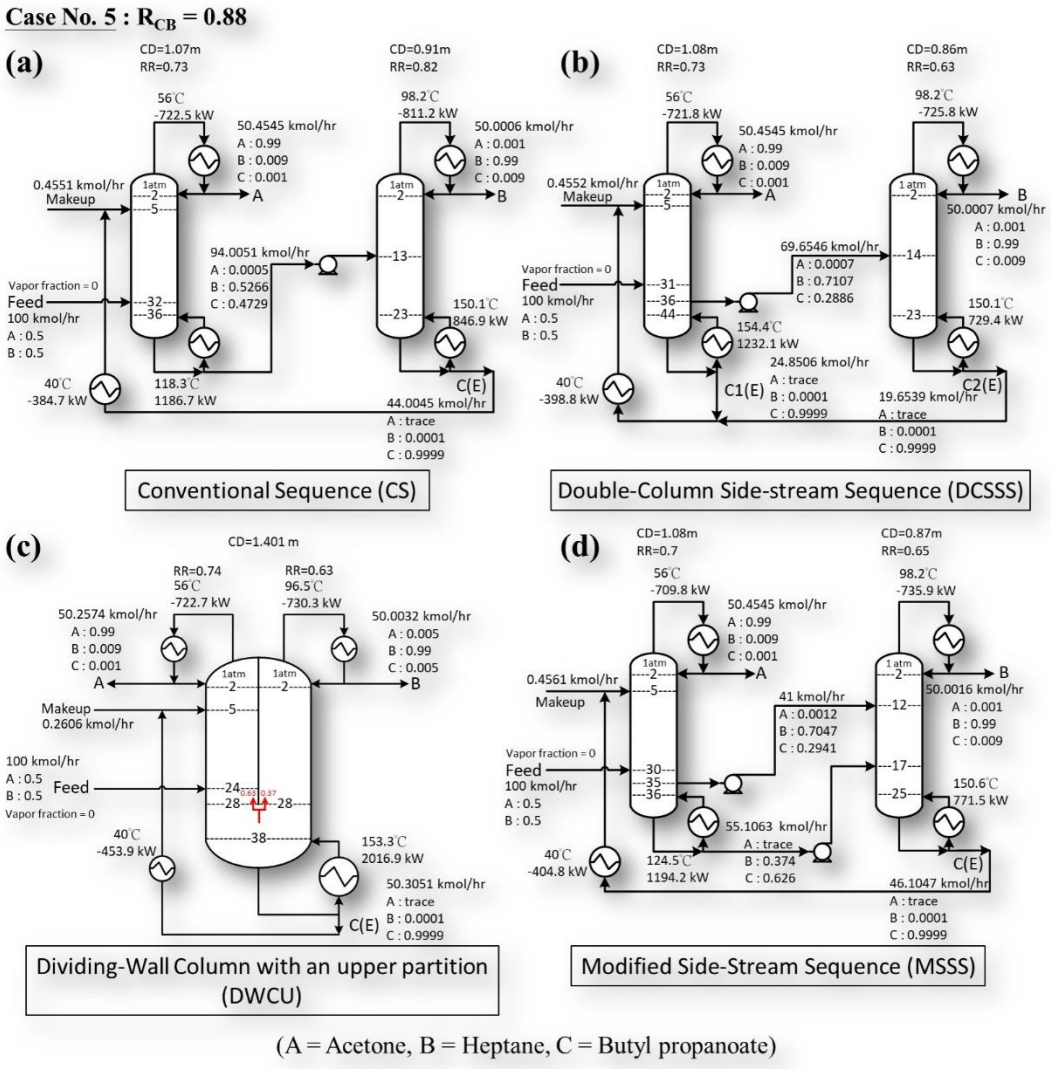

Figure 11. The detailed flowsheets for the optimized sequences for Case No.5

For the second column, the proper feed location can be determined by checking for a small extent of feed mismatch between the feed stream and feed stage [7]. Regarding the initial guess for column pressure, it is typically set to atmospheric pressure. At this point, the only remaining initial guess for the conventional sequence is the entrainer flow rate. Figure 12 shows the variation of TAC at different fixed entrainer flow rates, with all other variables optimized during the first phase of optimization. The lower bound of the

doi:10.6342/NTU202301003

entrainer flow rate in Figure 12 is around 40 kmol/hr because the mixtures of A/B will exhibit azeotropic behavior if the flow rate decreases further. A suitable initial guess for the entrainer flow rate should be 45 kmol/hr, as a local minimum occurs in this region. This local minimum serves as the initial variables for the second phase of optimization. The variables of the local minimum are optimized again using a smaller step size in the entrainer flow rate to obtain the final optimization results. After the second phase of optimization, the trend in Figure 12 can be used to verify the result. The final optimized entrainer flow rate should lie between 40 and 50 kmol/hr.

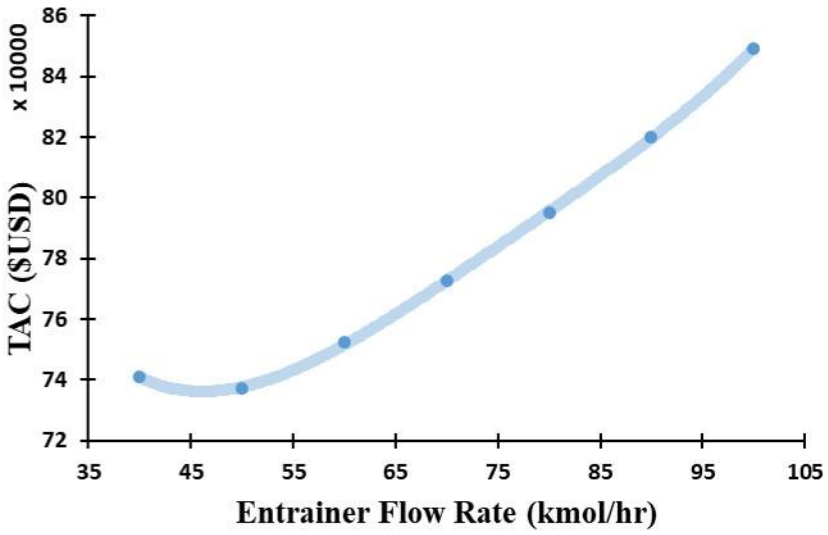

Figure 12. TAC versus the variation of the entrainer flow rate for the conventional sequence for Case No. 5, with other variables optimized.

The side stream flow rate of the MSSS is another critical variable that requires careful consideration during the optimization process. This variable must be optimized at different fixed entrainer flow rates and side stream flow rates, as demonstrated in Figure 13. Based on the results presented in Figure 13, suitable initial guesses for the entrainer

doi:10.6342/NTU202301003

flow rate should be around 45 kmol/hr and the side stream flow rate must be within the ranges of 35-55 kmol/hr, respectively. These curves can also be utilized to verify the final optimized values.

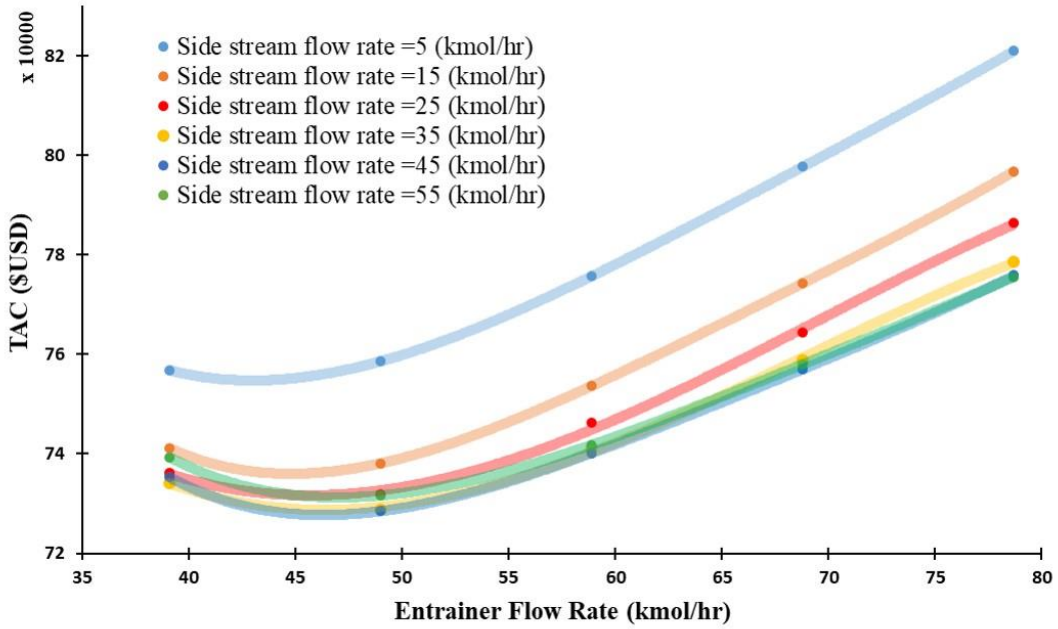

Figure 13. The variation of TAC at different side stream flow rate and entrainer flow rate for MSSS for Case No. 5, with other variables optimized.

The vapor split ratio of DWCU is another crucial variable that requires careful consideration during optimization. Figure 14 shows the TAC of DWCU with varying vapor split ratios while keeping other design variables fixed. The vapor split ratio has a more significant impact on the objective function than other variables of DWCU; therefore, the other variables are held constant during the first phase of optimization. In this case, an appropriate initial guess for the vapor split ratio is around 0.8. By comparing the optimized value of the vapor split ratio from the second phase of optimization with the results from the first phase, the validity of the final results can be confirmed. It's worth

doi:10.6342/NTU202301003

mentioning that not every case can produce such a complete curve as shown in Figure 14 because of convergence problems, which is why the example taken for the split ratio is no longer Case No.5 but rather Case No.9.

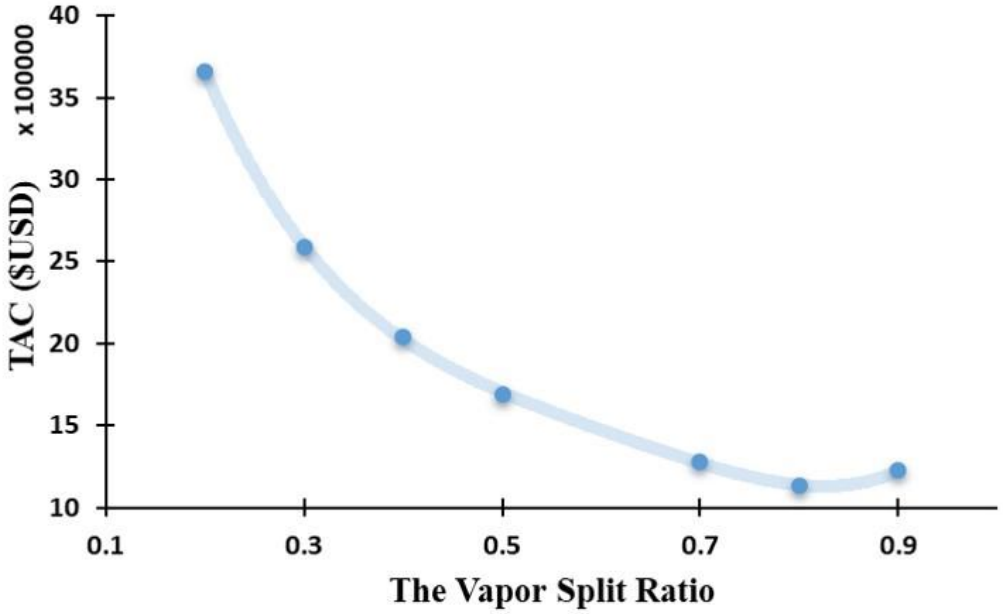

Figure 14. The variation of TAC at different vapor split ratios for Case No.9, with other variables fixed.

With the above-mentioned two-phase optimization, not only does the 2nd phase of optimization have better initial guesses, but also the final optimized variables can be verified by the results from the 1st phase, helping the optimization process converge more easily and making the final results more reliable.

doi:10.6342/NTU202301003

Chapter 3 The Interpretation of R_{CB}

R_{CB} has multiple interpretations (it affects the tradeoff between energy saving strategies in multiple ways). Five such interpretations are discussed in this chapter. The value of R_{CB} for each chemical system is determined from the values of the flowrate of species B (the heavy key) and C (the entrainer) in the optimized conventional sequence (CS).

3.1 The 1st Interpretation of R_{CB}

The first interpretation is that R_{CB} is a measure of the effectiveness of the entrainer similar to R_{EF}. Figure 15 illustrates the relation between R_{EF} and R_{CB} for six entrainers for the separation of methanol (MeOH) and dimethyl carbonate (DMC). The data for calculating R_{EF} and R_{CB} is taken from Hu and Cheng [34], who optimized the conventional sequence for separating MeOH/DMC with six different entrainers. In Figure 15, R_{EF} decreases as the R_{CB} decreases, showing that a smaller value of R_{CB} indicates a more effective entrainer.

doi:10.6342/NTU202301003

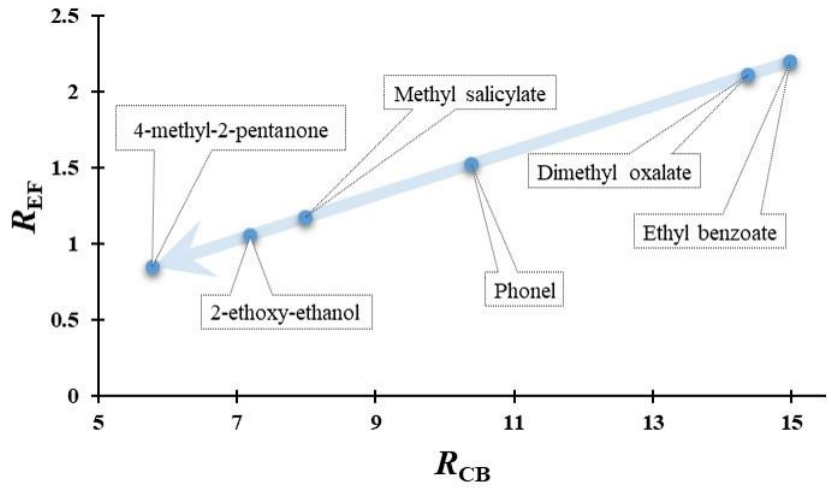

Figure 15. The relationship between the optimized entrainer-feed flow rate ratio (R_{EF}) and R_{CB} for the mixture MeOH/DMC separated by six different entrainers using the conventional sequence. The data is taken from Hu and Cheng [34].

3.2 The 2nd Interpretation of R_{CB}

The second interpretation of R_{CB} is an indicator of the extent of the remixing, defined as the maximum concentration of component B in the 1st column minus the composition of component B at the bottom of the 1st column. Figure 16 shows the relationship between R_{CB} and the extent of the remixing. The extent of remixing increases with increasing R_{CB}.

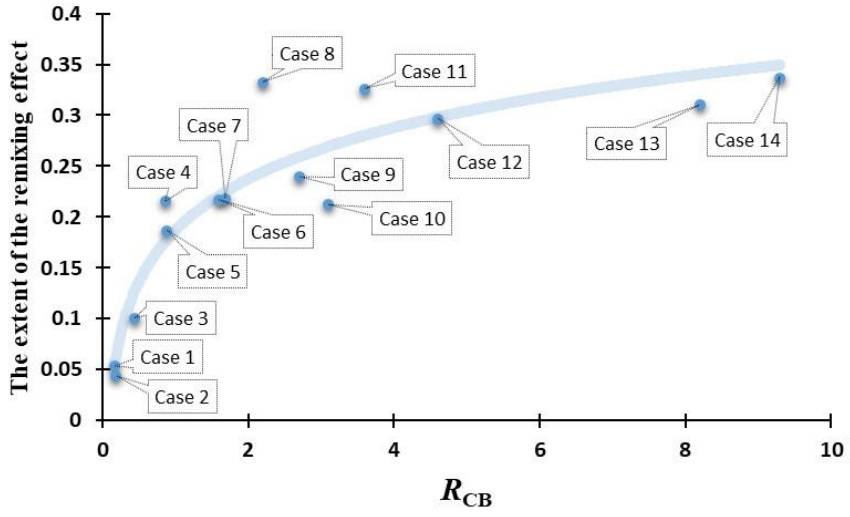

Figure 16. The relation between the extent of the remixing effect (in the optimized conventional sequence) and R_{CB} for chemical systems with effective entrainers where remixing is a concern (mixtures 1–14).

doi:10.6342/NTU202301003

This trend makes sense because as R_{CB} increases, there is more entrainer diluting species B at the bottom of the extractive column. This lowers the concentration of species B at the bottom of the column but has less effect on the peak concentration of B partway down the column, as shown in Figure 17. Thus the remixing as quantified by the difference between the peak concentration and the bottom concentration becomes worse. A greater remixing effect usually makes side-stream sequences and the dividing-wall column preferable since these design alternatives can mitigate the remixing effect.

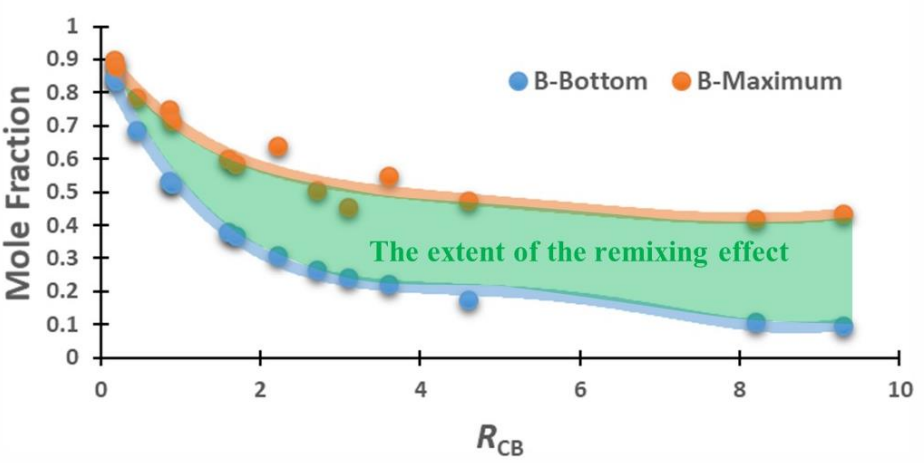

Figure 17. The maximum and the bottom concentration of component B in the 1st column versus R_{CB}

3.3 The 3rd Interpretation of R_{CB}

The third interpretation is a measure of the concentration of entrainer at the bottom of the 1st column. As R_{CB} increases, the concentration of the entrainer at the bottom of the extractive column (X_C) increases, making it easier to recover high-purity entrainer at the bottom of the 1st column. Figure 18 shows the relation between X_C and R_{CB}. If R_{CB} is low, then X_C is low and more energy is required to recover entrainer with high purity at the

doi:10.6342/NTU202301003

bottom of the 1st column. By contrast, if R_{CB} is high, then Xc is high and it is easier to recover high-purity entrainer at the bottom of the 1st column. The value of R_{CB} gives an indication of which of the alternatives shown in Figure 18 (MSS or DCSS) is likely to be preferable.

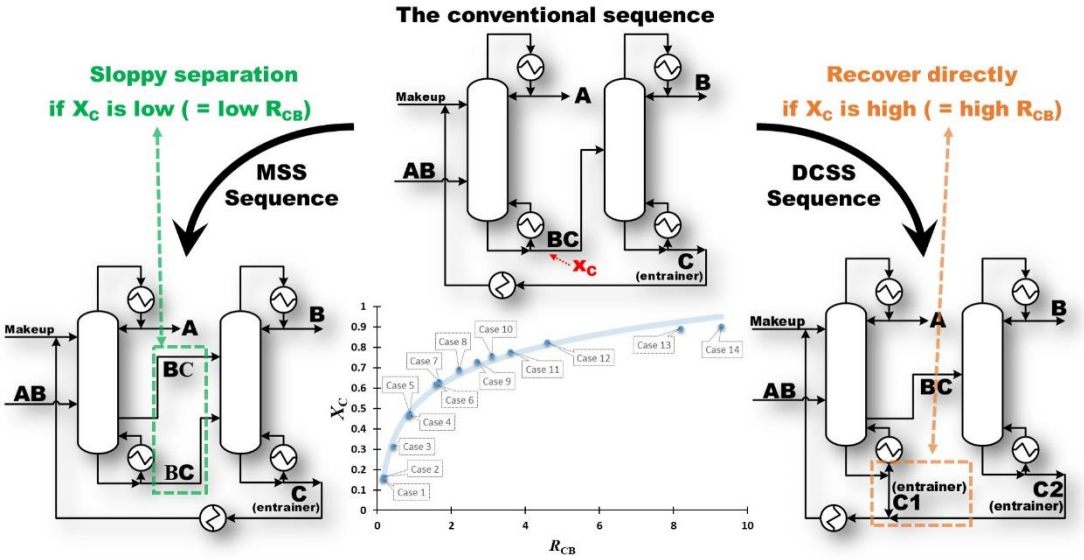

Figure 18. The concentration of the entrainer at the bottom of the 1st column (X_C) versus R_{CB}, where X_c refers to the entrainer composition at the bottom stream of the extractive column after optimization, as shown in the figure.

3.4 The 4th Interpretation of R_{CB}

The fourth interpretation of R_{CB} is as an indicator of the temperature difference between the 1st reboiler and the 2nd condenser. This is the barrier that must be overcome by adjusting the column pressures in order to implement column stacking. Two factors determine whether column stacking is feasible or not. One is that the normal boiling point of the entrainer cannot be too high compared to that of the heavy key, and the other is the amount of entrainer at the bottom of the 1st column. Because one criteria for a good entrainer is that it is easy to recover, the boiling point of the entrainer should never be too

doi:10.6342/NTU202301003

close to that of the heavy key. This means that the amount of the entrainer at the bottom of the 1st column is the most crucial factor. Figure 19 shows the variation of the temperature difference for different values of R_{CB}. As R_{CB} increases, the temperature of the 1st reboiler becomes higher because the concentration of the entrainer at the bottom rises, making stacking more difficult.

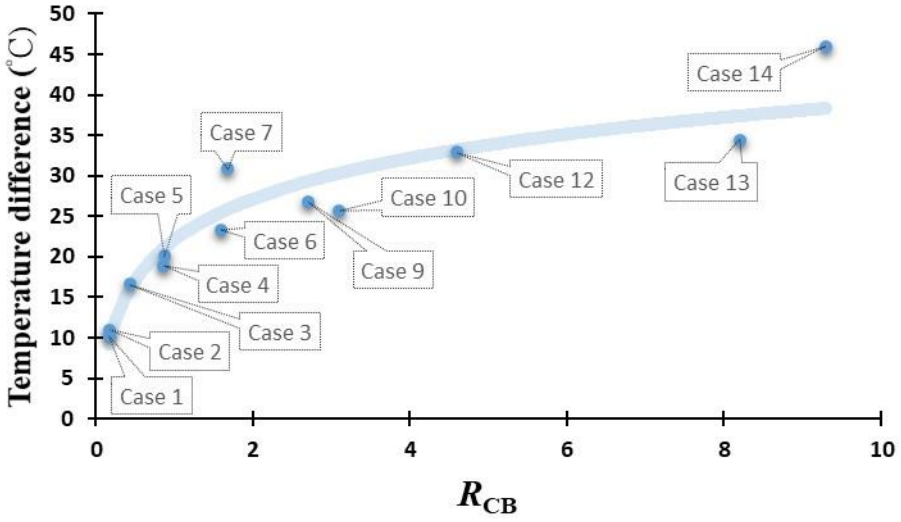

Figure 19. The temperature difference ΔT that must be overcome to implement column stacking versus R_{CB} for mixtures where column stacking is feasible (mixtures 1–7, 9,10, 12–14), where ΔT refers to the temperature difference between the 1st reboiler and the 2nd condenser of the optimized conventional sequence.

3.5 The 5th Interpretation of R_{CB}

The last physical meaning of R_{CB} is the difference in energy requirement between the 1st reboiler and the 2nd condenser. The duty difference in percentage here refers to the duty of the 2nd condenser divided by that of the 1st reboiler. If it approaches 100%, the top vapor can provide all of the energy for the 1st reboiler as long as the required driving force for heat exchange is satisfied. By contrast, if the percentage approaches zero, column

doi:10.6342/NTU202301003

stacking is not attractive since the top vapor of the 2nd column provides little energy to the 1st reboiler. The duty difference is plotted vs. R_{CB} in Figure 20. The duty difference increases with increasing R_{CB}. This can be understood for two reasons. First, for a given chemical system, a relatively large value of R_{CB} may indicate that the entrainer in that chemical system performs less well than the entrainers in other systems. This increases the duty in the extractive column more than the recovery column. A large value of R_{CB} may also be due to the fact that the concentration of B in the feed is relatively small. For example, a chemical system with an equimolar feed (0.5/0.5) is expected to have a smaller value of R_{CB} than the same system where the feed is enriched in species A (0.8/0.2) because the flowrate of B (in the denominator of the ratio) is larger. If the concentration of species B in the feed is small, this increases the duty of the extractive column and decreases the duty of the recovery column. A few examples with detailed flowsheets are provided in Appendix F.

doi:10.6342/NTU202301003

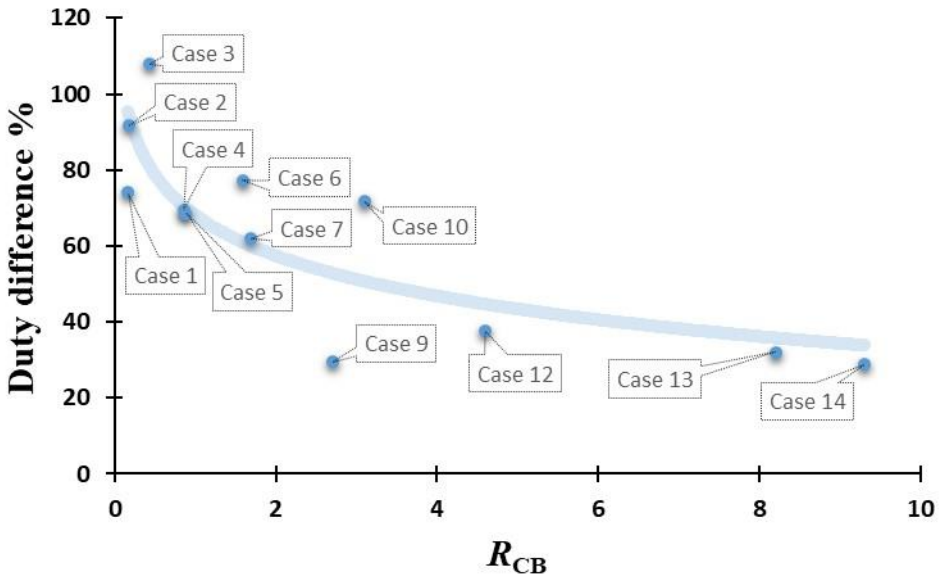

Figure 20. The duty difference as a percentage (the duty of the 2nd condenser/the duty of the 1st reboiler) in the optimized conventional sequence versus R_{CB} for mixtures for which column stacking is feasible (mixtures 1–7, 9,10, 12–14)

doi:10.6342/NTU202301003

Chapter 4 Results

This chapter shows the best sequence of each case with and without considering column stacking, and discusses the phenomena observed from the optimization results, drawing several conclusions.

4.1 Results for Sequences with no Column Stacking

Results for sequences without column stacking, including CS, CS-PRE, DCSSS, MSSS, and DWCU, are given in this section. Column stacking cannot be applied to DWCU because it has only one shell, so the operating pressures of different sections cannot be adjusted independently. Column stacking can be applied to the other sequences and will be discussed in Chapter 4.2.

4.1.1 The Preferred Non-stacked Sequence for Each Case

Figure 21 shows the best non-stacked sequence on a number line indicating the value of R_{CB}. Each dot represents a different azeotropic system with a different value of R_{CB}, where the numbers in black, green, and red represent the value of R_{CB}, cost savings (TAC), and energy savings (reboiler duty Q), respectively. Percentages are calculated based on the conventional sequence. The values of TAC and Q for every sequence without stacking for each azeotropic system is given in Appendix E. Starting from small values of R_{CB} on the left, MSSS is the preferred sequence without stacking for all azeotropic systems until a transition somewhere between R_{CB}=8.2 and R_{CB}=9.3, after which DCSSS is preferred.

doi:10.6342/NTU202301003

The transition point is estimated to be approximately 8.4 as shown in Figure 22, where TAC savings are plotted versus R_{CB} for both MSSS and DCSSS. DWCU is never preferred. (MSSS or DCSSS performs better for all azeotropic systems considered.)

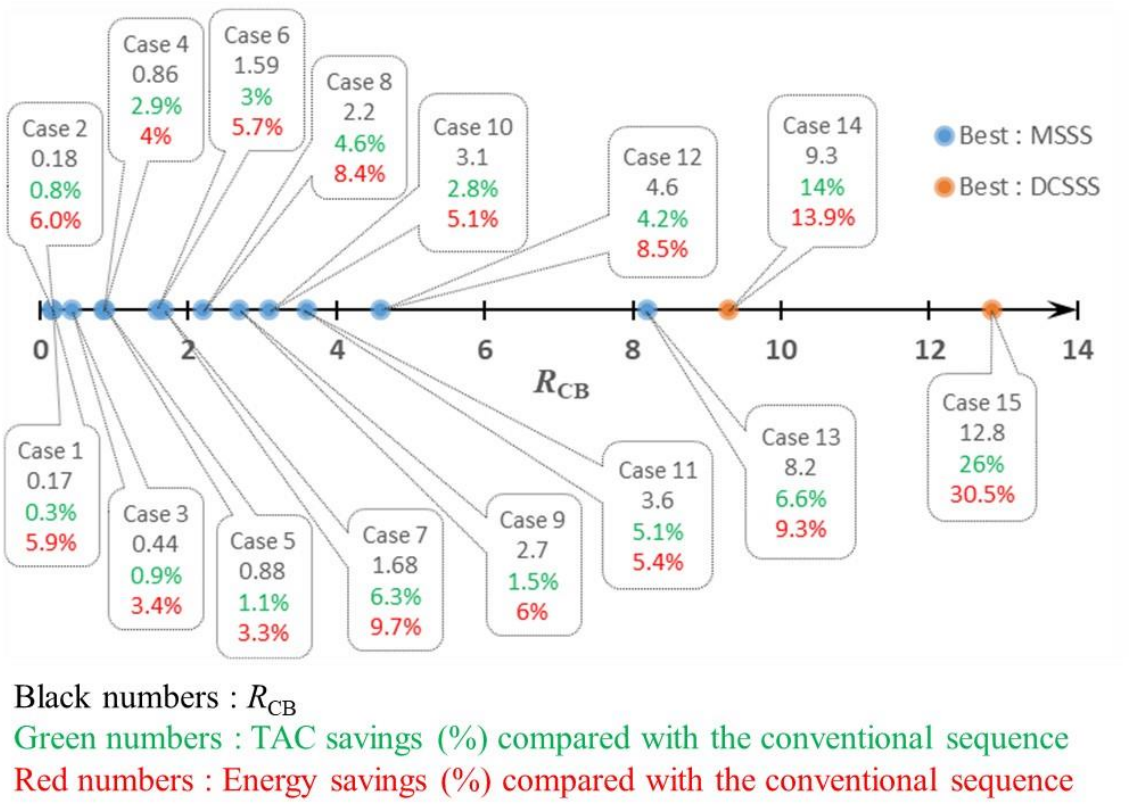

Figure 21. The best non-stacked sequence versus R_{CB}. Non-stacked sequences include CS-PRE, DCSSS, MSSS, and DWCU. MSSS is preferred when R_{CB} is relatively small; DCSSS is preferred when R_{CB} is relatively large. CS-PRE and DWCU are not preferred for any of the mixtures considered in this work.

doi:10.6342/NTU202301003

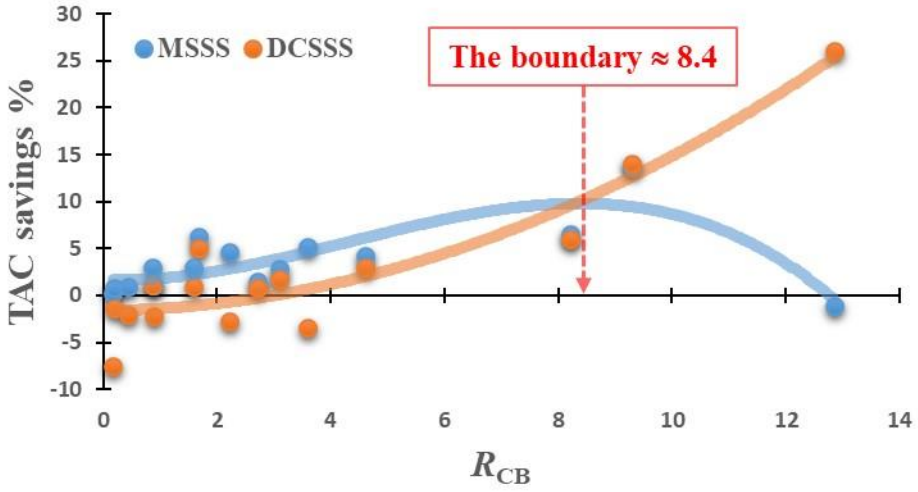

Figure 22. The trend of TAC savings % (sequences without stacking) versus R_{CB}

4.1.2 Examples with Detailed Flowsheets for Non-stacked Sequences

To understand the tradeoff between alternative sequences as R_{CB} changes, two azeotropic systems are chosen for comparison, cases No. 7 (methanol/vinyl acetate/allyl acetate, R_{CB}=1.68) and No. 14 (ethyl acetate/heptane/xylene, R_{CB}=9.3). Figure 23 shows the conventional sequence and the best unstacked alternative, MSSS, for separating a mixture of methanol and vinyl acetate using allyl acetate as the entrainer. Since R_{CB} is small (1.68), a smaller extent of remixing is expected in the first column of the conventional sequence. Furthermore, because the entrainer is not expected to be in substantial excess at the bottom of the entrainer column, it is likely not a suitable strategy to recover high-purity entrainer at the bottom of the 1st column. Instead, the bottom stream (rich in the entrainer allyl acetate) and the side stream (rich in the heavy key vinyl acetate) should both be routed to stages in the entrainer recovery column with similar

doi:10.6342/NTU202301003

compositions. In this way the remixing effect is mitigated.

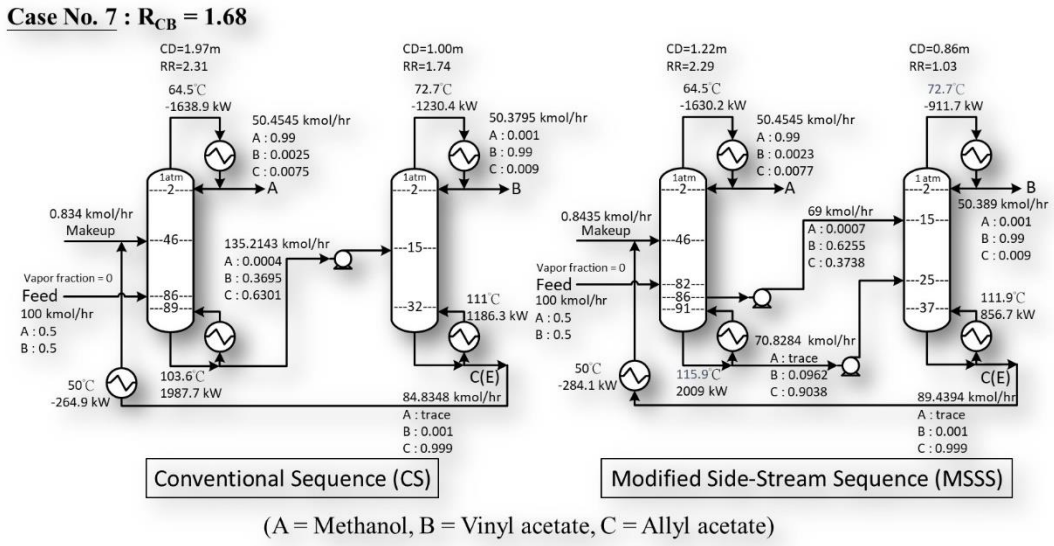

Figure 23. The conventional sequence (left) and the best alternative (right) for case No. 7

By contrast, for case No. 14, DCSSS is preferred. The different outcome can be understood in terms of R_{CB}. Figure 24 shows the optimized conventional sequence and the optimized best sidestream sequence, DCSSS, for azeotropic mixture No. 14 (Ethyl acetate/heptane/p-xylene). Because the value of R_{CB} is large, it is expected that the remixing effect will be substantial and that the bottom stream will consist mostly of entrainer. Therefore, recovering some of the entrainer at the bottom of the 1st column at high purity is a reasonable strategy. Because most of the entrainer leaves at the bottom of the 1st column and only a small amount of entrainer flows into the 2nd column, the throughput of the 2nd column decreases drastically, reducing the duty and the column diameter.

Another interesting phenomenon is that the entrainer flow rate in the optimized

doi:10.6342/NTU202301003

DCSSS flowsheet is even greater than that of the conventional sequence. The higher entrainer flow rate contributes to the lower duty of the extractive column because the relative volatility of the light key over the heavy key becomes higher. However, an increase in the entrainer flow rate also causes the duty of the recovery column to be higher. Therefore, when the entrainer flow rate is increased or decreased, a tradeoff between the heat duty of the extractive column and the recovery column arises [55]. By removing most of the entrainer from the bottom of the extractive column, DCSSS can achieve a lower duty in the extractive column by raising the entrainer flow rate without increasing the duty of the recovery column. For these reasons DCSSS performs the best for this mixture.

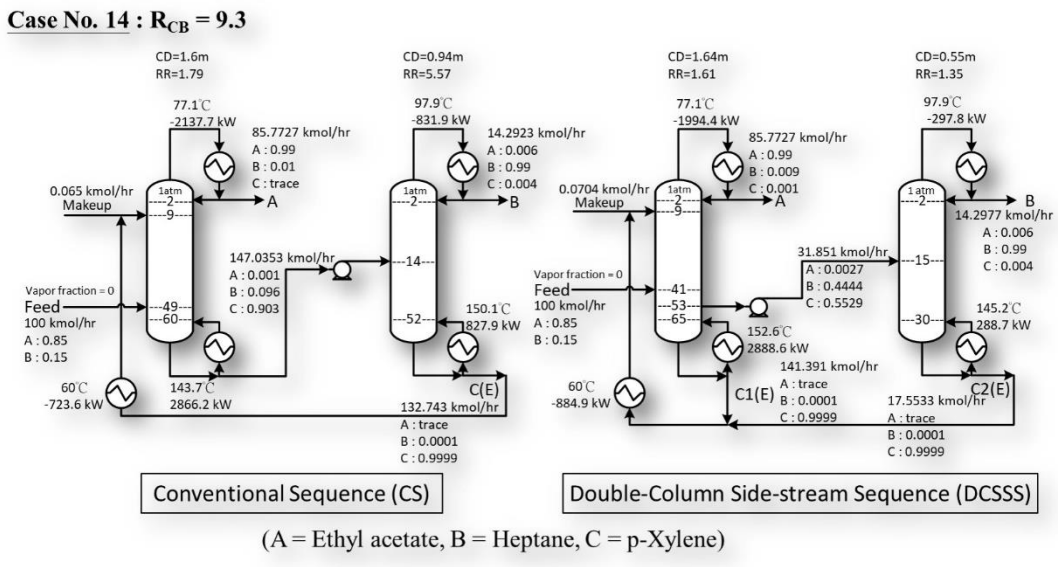

Figure 24. The conventional sequence (left) and the best alternative (right) for case No. 14

Even though side-stream sequences can mitigate the remixing effect, they are not

doi:10.6342/NTU202301003

always beneficial because of another important factor, the relative volatility of B (heavy key) to C (entrainer). In this work, α_{BC} refers to the average relative volatility of B/C over all the stages in the recovery column. The higher the value of α_{BC}, the easier it is to separate B and C. As α_{BC} increases, a sidestream is less beneficial because the separation of B and C is easier. At the same time, there is a disadvantage of implementing sidestreams, which is that the reboiler temperature in the first column increases because there is less of species B at the bottom of the column. As a result, there is a tradeoff between lessening the remixing effect and increasing the operating temperature of the 1st reboiler.

As shown in Table 4, R_{CB} for cases No. 16 and No. 17 are 5.19 and 4.09, indicating that the remixing effect is significant. However, the values of α_{BC} in these two cases are 32.01 and 36.54, respectively. The high value of α_{BC} makes a sidestream ineffective at reducing cost and energy consumption for these mixtures. A side stream doesn't significantly reduce the heat duty of the recovery column but does increases the temperature of the reboiler in the 1st column. Therefore, the side-stream sequences perform worse than the conventional sequence.

doi:10.6342/NTU202301003

Table 4. The best sequence for different R_{CB} and α_{BC}

Case No.	R_{CB}	Average α_{BC}	TAC savings % of the best side-stream sequence	The best sequence
1	0.17	5.00	0.3%	MSSS
2	0.18	2.87	0.8%	MSSS
3	0.44	2.13	0.9%	MSSS
4	0.86	4.44	2.9%	MSSS
5	0.88	3.95	1.1%	MSSS
6	1.59	4.89	3.0%	MSSS
7	1.68	2.71	6.3%	MSSS
8	2.21	6.24	4.6%	MSSS
9	2.70	2.34	1.5%	MSSS
10	3.10	4.85	2.8%	MSSS
11	3.60	20.02	5.1%	MSSS
17	4.09	36.54	-5.8%	CS
12	4.60	5.34	4.2%	MSSS
16	5.19	32.01	-0.6%	CS
13	8.20	5.49	6.6%	MSSS
14	9.30	3.27	14.0%	DCSSS
15	12.80	3.12	26.0%	DCSSS

The TAC savings of the best side-stream sequence with different R_{CB} and α_{BC} can be estimated by regression, as shown in Figure 25. A higher value of R_{CB} and a smaller value of α_{BC} lead to a higher TAC savings by side-stream sequences, but this also indicates that the entrainer is less effective. In contrast, a smaller R_{CB} and a larger α_{BC} lead to lower TAC savings, suggesting that the entrainer performs well. As a result, both R_{CB} and α_{BC} should be considered when predicting whether side-stream sequences are likely to be attractive.

doi:10.6342/NTU202301003

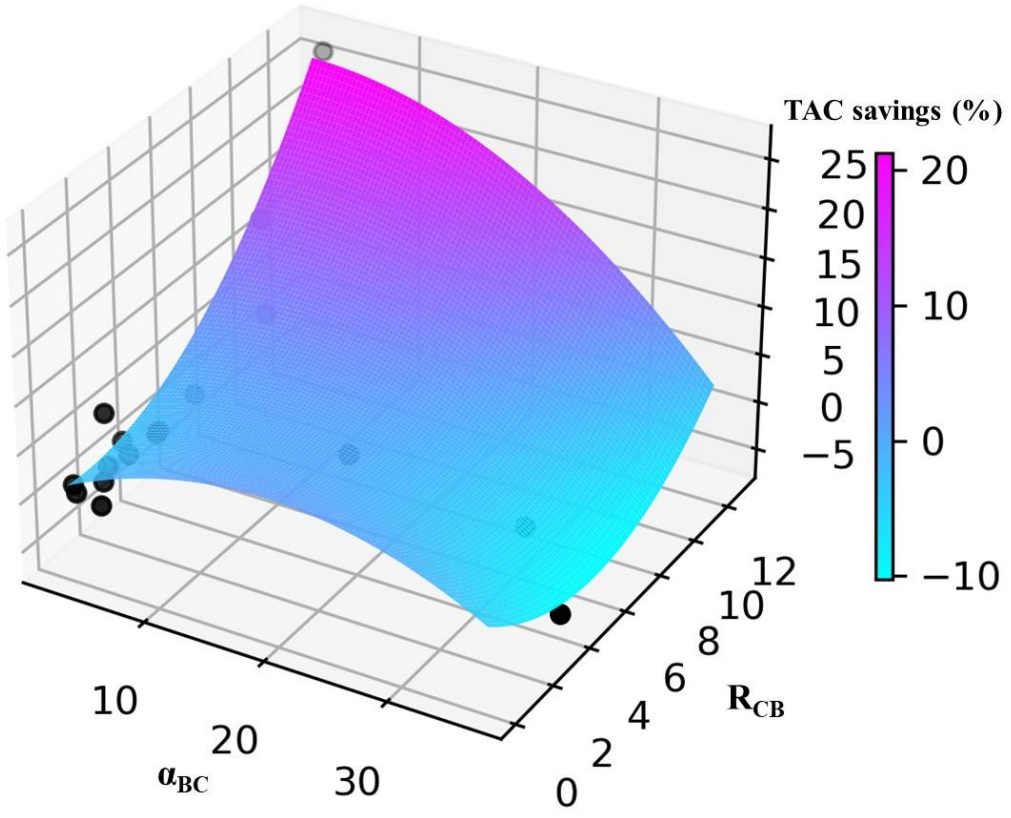

Figure 25. The variation of TAC savings for different R_{CB} and $\boldsymbol{\alpha_{BC}}$

In summary, the data collected in this work show that for sequences without column stacking, sequence MSSS is preferred for small values of R_{CB} (less than about 8.4) and DCSSS is preferred for larger values of R_{CB} (greater than about 8.4). However, the relative volatility of the heavy key and the entrainer (α_{BC}) is also a factor. If α_{BC} is very large, side-stream sequences may not be attractive.

4.2 Results for Sequences with Column Stacking

In this section, three stacked sequences, OSS, SMSSS, and SDCSSS are compared, and the conventional sequence is again taken as the base case.

doi:10.6342/NTU202301003

4.2.1 The Preferred Stacked Sequence for Each Case

Figure 26 shows the preferred stacked sequence on a number line indicating the value of R_{CB}. The black number is R_{CB}. The green and red percentages represent the improvement of TAC and energy consumption compared to the conventional sequence. Values of TAC and Q (the reboiler duty) for each stacked sequence are given in Appendix E. From Figure 26, the value of R_{CB} above which SDCSSS outperforms OSS is between 1.68 and 2.7. This point can be estimated more precisely by comparing the trend of TAC savings percentage of the two sequences, as shown in Figure 27. The transition point where the orange and blue lines cross is approximately 2.2. The gray line shows the difference in savings (on a percentage basis) between OSS and SDCSSS, plotted versus R_{CB}. Tututi et al. [21] also compared OSS, SDCSSS and CS for separating acetone and methanol with water as an entrainer (case No. 10, R_{CB}=3.1). Their results are consistent with the findings presented here.

doi:10.6342/NTU202301003

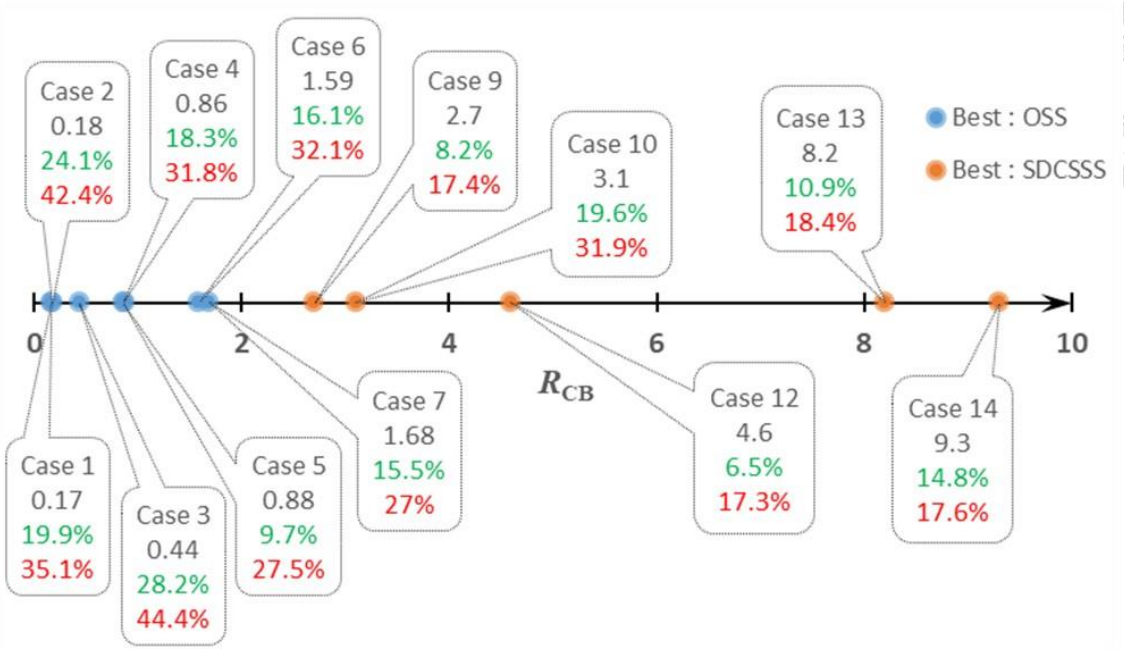

Black numbers : R_{CB}

Green numbers : TAC savings (%) compared with the conventional sequence

Red numbers : Energy savings (%) compared with the conventional sequence

Figure 26. The best stacked sequences versus R_{CB}

doi:10.6342/NTU202301003

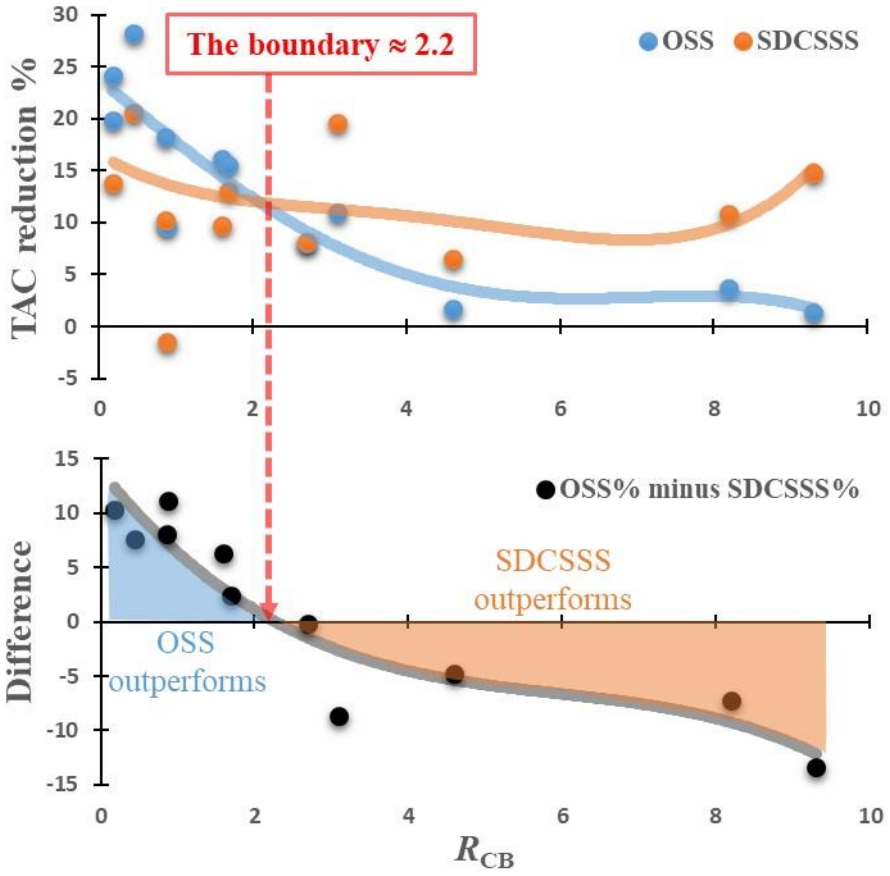

Figure 27. The trend of TAC savings % (Stacked sequences) versus R_{CB}

4.2.2 Examples with Detailed Flowsheets for Stacked Sequences

To explore the effect of R_{CB} on the choice between OSS and SDCSSS, two representative cases are selected, case No. 1 (methanol/toluene/butyl propanoate) for which OSS is preferred and case No. 13 (acetone/methanol/water) for which SDCSSS is preferred. Figure 28 shows the optimized base case conventional sequence (CS) and the best optimized stacked sequence OSS for separating methanol and toluene with butyl butanoate as entrainer (case No. 1). The value of R_{CB} for this mixture is 0.17. The small value of R_{CB} suggests that the entrainer is very effective, the remixing effect is minor, the

doi:10.6342/NTU202301003

temperature barrier for implementing column stacking is small, and the heat duty difference between the 2nd condenser and the 1st reboiler is not large. Because the remixing effect is minor, the benefit from a side stream is limited. A small temperature difference between the 1st reboiler and the 2nd condenser indicates that only a small change in column pressures will be required to achieve the necessary driving force for heat transfer. Furthermore, a small difference in heat duty means that most of the energy required for the 1st reboiler can be provided by the 2nd condenser, making column stacking attractive. For these reasons, OSS performs well for this chemical system with a small value of R_{CB}.

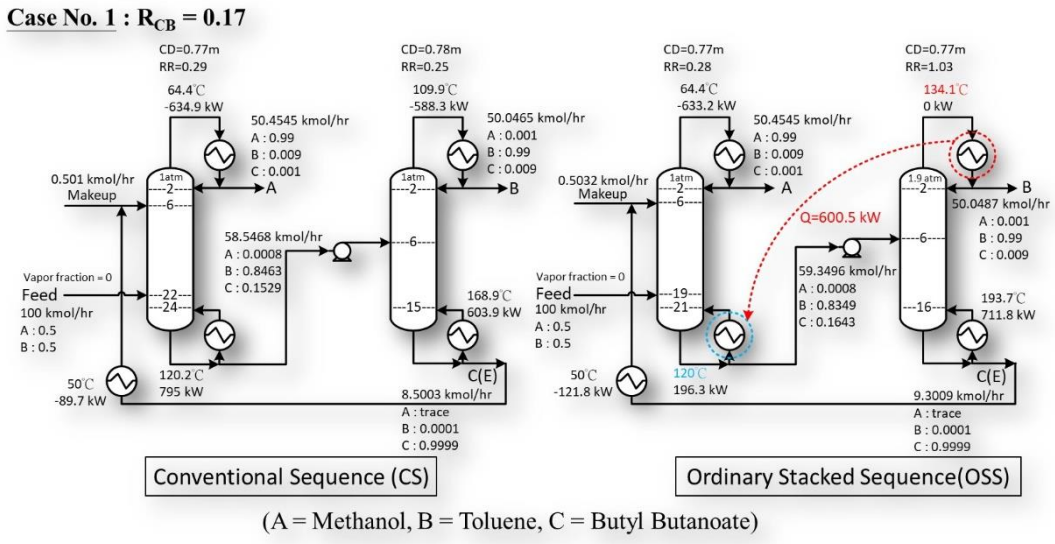

Figure 28. The conventional sequence (left) and the best alternative (right) for case No. 1

In contrast with case No.1, case No.13 has a much higher value of R_{CB}, R_{CB}=8.2. The larger value of R_{CB} suggests a more pronounced remixing effect, a high entrainer concentration at the bottom of the 1st column, a larger temperature difference to overcome,

doi:10.6342/NTU202301003

and a larger difference between the condenser duty and the reboiler duty. The situation is not ideal for implementing column stacking, but stacking can still reduce energy consumption without a prohibitive increase in the pressure of the 2nd column. As shown in Figure 29, SDCSSS saves 512.1 kW compared to the conventional sequence with acceptable increases in the duty of the cooler and the temperature of the 2nd reboiler. The increased cooler duty is due to the increased entrainer flow rate and the increased temperature of the 2nd reboiler. Increased entrainer flowrate is a characteristic and an advantage of SDCSSS (and DCSSS), as mentioned in the discussion of Figure 24 in Section 4.1.2. As for the increased temperature of the 2nd reboiler, it is an inevitable consequence of implementing column stacking. Increasing the pressure of the 2nd column also increases its column temperature, which further increases the duty of the cooler. Fortunately, this problem can be solved by another heat integration strategy, preheating, in which the sensible heat in the recycled entrainer is used to preheat the fresh feed. Although preheating is beyond the scope of this work, it should be considered for this flowsheet alternative.

As discussed in Chapter 4.1 the attractiveness of side-streams depends not only on the value of R_{CB} but also the value of α_{BC}. However, a large difference in the boiling points of B and C will make stacking infeasible. A moderate temperature difference between the boiling points of B and C generally corresponds to a moderate value of α_{BC},

doi:10.6342/NTU202301003

which is why relative volatility is often not a great concern if stacking is feasible. It is advantageous to combine column stacking with a side-stream sequence because both stacking and the side stream reduce energy consumption at this value of R_{CB}, which explains why SDCSSS outperforms all other alternatives.

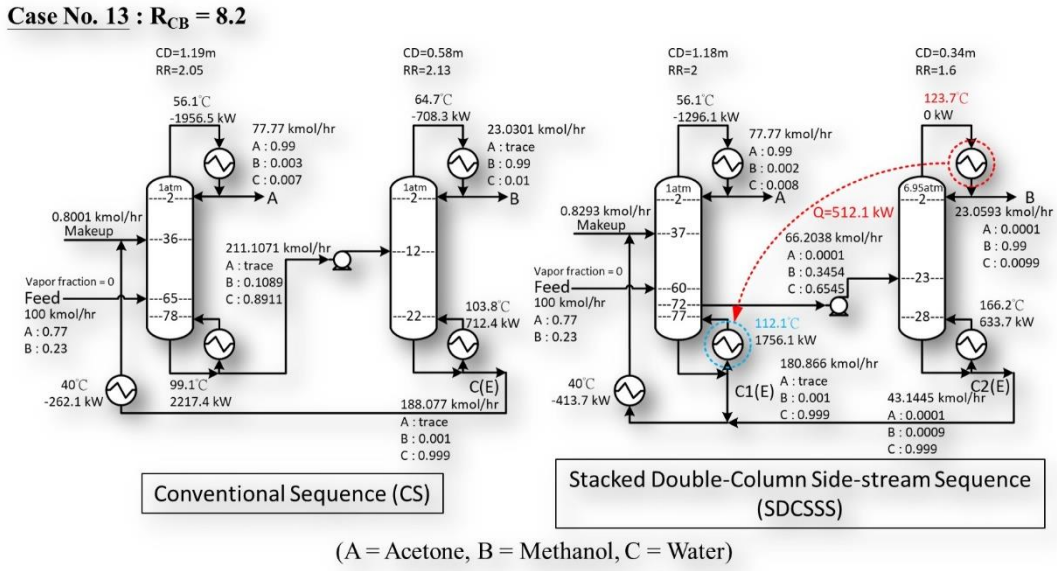

Figure 29. The conventional sequence (left) and the best alternative (right) for case No. 13

In summary, applying column stacking to a side-stream sequence is sometimes beneficial and sometimes not. The data suggest that if column stacking is feasible and R_{CB}<2.2, OSS is recommended; if column stacking is feasible and R_{CB}>2.2, SDCSSS is recommended.

doi:10.6342/NTU202301003

4.3 Overall Evaluation

In this section, all strategies are compared to present an overall view of the results.

4.3.1 The Dividing Wall versus Side Streams

Figure 30 shows the performance of the side stream sequences and the thermally coupled sequence in terms of cost reduction and energy savings versus R_{CB}. The conventional sequence still serves as the base case for each case. When R_{CB} is high, indicating that the remixing effect is severe, DWCU becomes economical as shown in Figure 30(a). This is consistent with the results of Wu et al. [56]. Figure 30 (b) shows that DWCU is more effective at decreasing energy consumption than cost, which is consistent with the findings of Cordeiro et al. [57]. The data collected in this work indicates that the best side-stream sequence in each case is always better than DWCU for both cost reduction and energy conservation unless R_{CB} is very high. However, a very large value of R_{CB} suggests that the entrainer performs poorly. In this case it may be preferable to seek a better entrainer or a different method of breaking the azeotrope.

doi:10.6342/NTU202301003

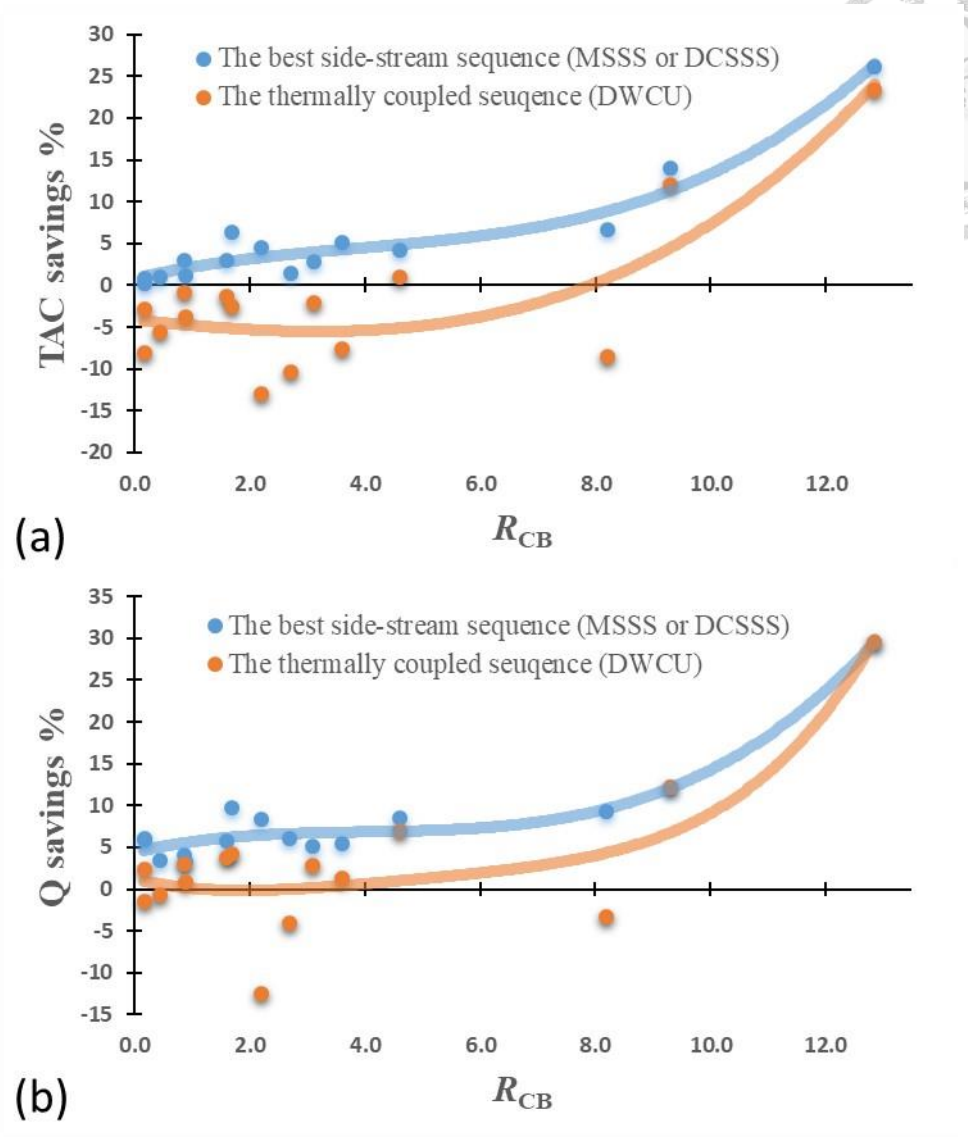

Figure 30. The side-stream sequences and the thermally coupled sequence versus R_{CB} (a) TAC savings and (b) reboiler duty Q savings

The finding that DWCU is less attractive than other options is somewhat at odds with the findings of Anokhina and Timoshenko [27], who found that the partially thermally coupled sequence, (PCEDS) which is the parent sequence of DWCU, can save energy when the reflux ratio in the extractive distillation sequence is greater than 1. The most likely reason for the discrepancy is that Anokhina and Timoshenko optimized their processes using energy consumption as the objective function, whearas in this work the

doi:10.6342/NTU202301003

total annual cost (including both capital and operating costs) is used as the objective function. As stated previously, DWCU and other thermally coupled sequences are more effective at reducing energy consumption than cost.

4.3.2 Column Stacking versus Side Streams

Although stacked side-stream sequences usually perform better than the ordinary sequence, they are not always the best choice. In Figure 31, the blue, orange, and gray lines represent the cost savings from side-stream sequences, column stacking, and stacked side-stream sequences respectively for different values of R_{CB}. Column stacking (the stacked-only sequence OSS) has the lowest cost when R_{CB} is low, whereas the side-stream sequence (no stacking) is less expensive when R_{CB} is high. The performance of column stacking (the orange line) is nearly the same as the best stacked side-stream sequence (the gray line) for small R_{CB}. Conversely, the performance of the best side-stream sequence (the blue line) is almost the same as the best stacked side-stream sequence when R_{CB} is large. This suggests that combining column stacking and a side stream is effective only for an intermediate range of values of R_{CB}. This range can be estimated from the intersections labeled in Figure 31. The lower bound is approximately R_{CB}=2.6 and the upper bound is approximately R_{CB}=8.4. Within this range, the combination of column stacking and a side-stream is likely to be most cost-effective. Below this range, the benefit of a side-stream is small and above this range the benefit of column stacking is small.

doi:10.6342/NTU202301003

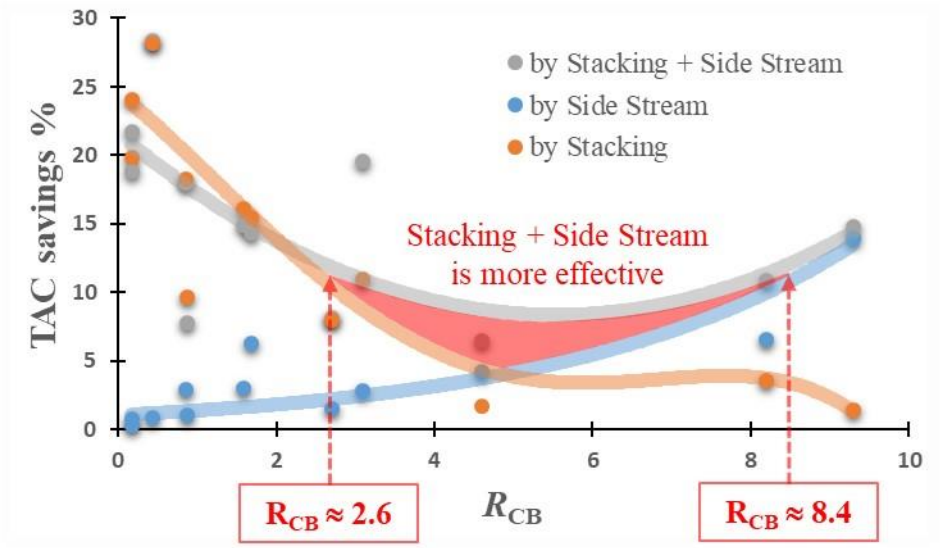

Figure 31. The effective range of applying stacking to the side-stream sequence according to R_{CB}

doi:10.6342/NTU202301003

Chapter 5 Conclusions

Three process intensification strategies for extractive distillation with a heavy entrainer are studied in this work, including thermal coupling, side streams, and column stacking. These three strategies are represented by six intensified sequences. A novel index R_{CB} is proposed for understanding the tradeoff between these alternatives. The data for the relative cost of design alternatives can be understood in terms of this index. The following conclusions can be drawn for the mixtures studied in this work based on the data: (1) Without column stacking, if R_{CB} is less than about 8.4, the modified side-stream sequence (MSSS) performs better; if R_{CB} is greater than 8.4, the double-column side-stream sequence (DCSSS) performs better. (2) Even if the remixing effect is severe (R_{CB} is high), the side-stream sequences may still be uneconomical if the relative volatility of the heavy key (B) and the entrainer (C) is too high. (3) With regard to column stacking, if R_{CB} is less than about 2.2, the ordinary stacked sequence (OSS) performs better; if R_{CB} is greater than about 2.2, the stacked double-column side-stream sequence (SDCSSS) performs best. (4) Column stacking is more effective when R_{CB} is small, and side-stream sequences are more effective when R_{CB} is large. (5) There is a range of values with R_{CB} greater than about 2.6 and less than about 8.4 where stacked side-stream sequences are recommended. When R_{CB} is less than about 2.6, the benefit of a side-stream is minimal and a sequence with only stacking is likely to be preferred for simplicity. Conversely,

doi:10.6342/NTU202301003

when R_{CB} is greater than about 8.4, the benefit of stacking is usually minimal and a sequence with only a side-stream is likely to be preferred for simplicity. (6) The dividing-wall column with an upper partition (DWCU) is not economical when R_{CB} is small and is economical but less attractive than side-stream sequences when R_{CB} is large.

doi:10.6342/NTU202301003

REFERENCES

1. Laroche, L., N. Bekiaris, H.W. Andersen, and M. Morari, *Homogeneous azeotropic distillation: separability and flowsheet synthesis.* Industrial & engineering chemistry research, 1992. **31**(9): p. 2190-2209.
2. Sholl, D.S. and R.P. Lively, *Seven chemical separations to change the world.* Nature, 2016. **532**(7600): p. 435-437.
3. Kiss, A.A. and R. Smith, *Rethinking energy use in distillation processes for a more sustainable chemical industry.* Energy, 2020. **203**: p. 117788.
4. Glinos, K.N., I.P. Nikolaides, and M.F. Malone, *New complex column arrangements for ideal distillation.* Industrial & Engineering Chemistry Process Design And Development, 1986. **25**(3): p. 694-699.
5. Agrawal, R. and Z.T. Fidkowski, *Are thermally coupled distillation columns always thermodynamically more efficient for ternary distillations?* Industrial & engineering chemistry research, 1998. **37**(8): p. 3444-3454.
6. Liu, Z., L. Hao, X. Han, Z. Cao, and H. Wei, *Novel energy saving and economic extractive distillation process via integrating two-feed preheating strategy and heat pump vapor recompression.* Separation and Purification Technology, 2023. **307**: p. 122791.
7. Cui, C., X. Zhang, and J. Sun, *Design and optimization of energy-efficient liquid-only side-stream distillation configurations using a stochastic algorithm.* Chemical Engineering Research and Design, 2019. **145**: p. 48-52.
8. Midori, S., S. Zheng, and I. Yamada, *Analysis of divided-wall column for extractive distillation; Suichoku bunkatsugata chushutsu joryuto ni kansuru kaiseki.* Kagaku Kogaku Ronbunshu, 2000. **26**.
9. Li, L., Y. Tu, L. Sun, Y. Hou, M. Zhu, L. Guo, Q. Li, and Y. Tian, *Enhanced efficient extractive distillation by combining heat-integrated technology and intermediate heating.* Industrial & Engineering Chemistry Research, 2016. **55**(32): p. 8837-8847.
10. Zhang, Q., M. Liu, C. Li, and A. Zeng, *Design and control of extractive distillation process for separation of the minimum-boiling azeotrope ethyl-acetate and ethanol.* Chemical Engineering Research and Design, 2018. **136**: p. 57-70.
11. Feng, Z., W. Shen, G. Rangaiah, and L. Dong, *Design and control of vapor recompression assisted extractive distillation for separating n-hexane and ethyl acetate.* Separation and Purification Technology, 2020. **240**: p. 116655.
12. Ma, Z., D. Yao, J. Zhao, H. Li, Z. Chen, P. Cui, Z. Zhu, L. Wang, Y. Wang, and Y. Ma, *Efficient recovery of benzene and n-propanol from wastewater via vapor recompression assisted extractive distillation based on techno-economic and*

doi:10.6342/NTU202301003

environmental analysis. Process Safety and Environmental Protection, 2021. **148**: p. 462-472.

13. Doherty, M.F. and M.F. Malone, *Conceptual design of distillation systems*. 2001, McGraw-Hill.
14. Abushwireb, F., H. Elakrami, and M. Emtir, *The effect of solvent selection on energy-integrated extractive distillation for aromatics recovery from pyrolysis gasoline: Simulation and optimization.* Chemical Engineering Transactions, 2009. **18**: p. 243-248.
15. Hernandez, S., *Analysis of energy-efficient complex distillation options to purify bioethanol.* Chemical Engineering & Technology: Industrial Chemistry-Plant Equipment-Process Engineering-Biotechnology, 2008. **31**(4): p. 597-603.
16. Errico, M., B.-G. Rong, G. Tola, and M. Spano, *Optimal synthesis of distillation systems for bioethanol separation. Part 2. Extractive distillation with complex columns.* Industrial & Engineering Chemistry Research, 2013. **52**(4): p. 1620-1626.
17. Cui, C., Q. Zhang, X. Zhang, J. Sun, and I.-L. Chien, *Process synthesis and plantwide control of intensified extractive distillation with preconcentration for separating the minimum-boiling azeotropes: A case study of acetonitrile dehydration.* Separation and Purification Technology, 2022. **285**: p. 120397.
18. Zhang, Q., A. Zeng, X. Yuan, and Y. Ma, *Design and control of economically attractive side-stream extractive distillation process.* Chemical Engineering Research and Design, 2020. **160**: p. 571-586.
19. Shi, T., W. Chun, A. Yang, Y. Su, S. Jin, J. Ren, and W. Shen, *Optimization and control of energy saving side-stream extractive distillation with heat integration for separating ethyl acetate-ethanol azeotrope.* Chemical Engineering Science, 2020. **215**: p. 115373.
20. Luyben, W.L., *Comparison of extractive distillation and pressure-swing distillation for acetone− methanol separation.* Industrial & engineering chemistry research, 2008. **47**(8): p. 2696-2707.
21. Tututi-Avila, S., N. Medina-Herrera, J. Hahn, and A. Jiménez-Gutiérrez, *Design of an energy-efficient side-stream extractive distillation system.* Computers & Chemical Engineering, 2017. **102**: p. 17-25.
22. Zhang, Y., A. Li, J. Gao, D. Xu, L. Zhang, Z. Zhang, and Y. Wang, *Thermal coupled extractive distillation sequences with three entrainers for the separation of azeotrope isopropyl alcohol+ diisopropyl ether.* Journal of Chemical Technology & Biotechnology, 2020. **95**(5): p. 1590-1603.
23. Xu, Y., J. Li, Q. Ye, and Y. Li, *Energy efficient extractive distillation process assisted with heat pump and heat integration to separate acetonitrile/1, 4-*

doi:10.6342/NTU202301003

dioxane/water. Process Safety and Environmental Protection, 2021. **156**: p. 144-159.

24. Yang, A., Z.Y. Kong, J. Sunarso, Y. Su, Q. Wang, and S. Zhu, *Insights on sustainable separation of ternary azeotropic mixture tetrahydrofuran/ethyl acetate/water using hybrid vapor recompression assisted side-stream extractive distillation.* Separation and Purification Technology, 2022. **290**: p. 120884.
25. Pleşu, V., A.E.B. Ruiz, J. Bonet, and J. Llorens, *Simple equation for suitability of heat pump use in distillation*, in *Computer Aided Chemical Engineering*. 2014, Elsevier. p. 1327-1332.
26. Gu, J., X. You, C. Tao, J. Li, W. Shen, and J. Li, *Improved design and optimization for separating tetrahydrofuran–water azeotrope through extractive distillation with and without heat integration by varying pressure.* Chemical Engineering Research and Design, 2018. **133**: p. 303-313.
27. Anokhina, E. and A. Timoshenko, *Criterion of the energy effectiveness of extractive distillation in the partially thermally coupled columns.* Chemical Engineering Research and Design, 2015. **99**: p. 165-175.
28. Gerbaud, V., I. Rodriguez-Donis, L. Hegely, P. Lang, F. Denes, and X. You, *Review of extractive distillation. Process design, operation, optimization and control.* Chemical Engineering Research and Design, 2019. **141**: p. 229-271.
29. Staak, D. and T. Grützner, *Process integration by application of an extractive dividing-wall column: An industrial case study.* Chemical Engineering Research and Design, 2017. **123**: p. 120-129.
30. Chen, Y.-Y., Z.Y. Kong, A. Yang, H.-Y. Lee, and J. Sunarso, *Design and control of an energy intensified side-stream extractive distillation for binary azeotropic separation of n-hexane and ethyl acetate.* Separation and Purification Technology, 2022. **294**: p. 121176.
31. Tang, W.-T. and J.D. Ward, *Energy and exergy analysis of a stacked complex sequence and alternatives for ternary distillation.* Separation and Purification Technology, 2023. **304**: p. 122384.
32. He, S., W. Fan, H. Huang, J. Gao, D. Xu, Y. Ma, L. Zhang, and Y. Wang, *Separation of the Azeotropic Mixture Methanol and Toluene Using Extractive Distillation: Entrainer Determination, Vapor–Liquid Equilibrium Measurement, and Modeling.* ACS omega, 2021. **6**(50): p. 34736-34743.
33. Matsuda, H., H. Takahara, S. Fujino, D. Constantinescu, K. Kurihara, K. Tochigi, K. Ochi, and J. Gmehling, *Selection of entrainers for the separation of the binary azeotropic system methanol+ dimethyl carbonate by extractive distillation.* Fluid Phase Equilibria, 2011. **310**(1-2): p. 166-181.
34. Hu, C.-C. and S.-H. Cheng, *Development of alternative methanol/dimethyl*

doi:10.6342/NTU202301003

carbonate separation systems by extractive distillation—A holistic approach. Chemical Engineering Research and Design, 2017. **127**: p. 189-214.

35. Arce, A., E. Rodil, and A. Soto, *Extractive distillation of 2-methoxy-2-methylpropane+ ethanol using 1-butanol as entrainer: Equilibria and simulation.* The Canadian Journal of Chemical Engineering, 1999. **77**(6): p. 1135-1140.
36. Zhang, T., A. Li, X. Xu, Y. Ma, D. Xu, L. Zhang, J. Gao, and Y. Wang, *Separation of azeotropic mixture (acetone+ n-heptane) by extractive distillation with intermediate and heavy boiling entrainers: Vapour-liquid equilibrium measurements and correlation.* The Journal of Chemical Thermodynamics, 2021. **152**: p. 106284.
37. Lladosa, E., J.B. Montón, M.C. Burguet, and R. Muñoz, *Effect of pressure and the capability of 2-methoxyethanol as a solvent in the behaviour of a diisopropyl ether–isopropyl alcohol azeotropic mixture.* Fluid phase equilibria, 2007. **262**(1-2): p. 271-279.
38. Luo, H., K. Liang, W. Li, Y. Li, M. Xia, and C. Xu, *Comparison of pressure-swing distillation and extractive distillation methods for isopropyl alcohol/diisopropyl ether separation.* Industrial & Engineering Chemistry Research, 2014. **53**(39): p. 15167-15182.
39. Resa, J.M., C. González, S.O. de Landaluce, and J. Lanz, *(Vapour+ liquid) equilibria, densities, excess molar volumes, refractive indices, speed of sound for (methanol+ allyl acetate) and (vinyl acetate+ allyl acetate).* The Journal of Chemical Thermodynamics, 2002. **34**(7): p. 1013-1027.
40. Zhang, Y., Z. Wang, X. Xu, J. Gao, D. Xu, L. Zhang, and Y. Wang, *Entrainers selection and vapour-liquid equilibrium measurements for separating azeotropic mixtures (ethanol+ n-hexane/cyclohexane) by extractive distillation.* The Journal of Chemical Thermodynamics, 2020. **144**: p. 106070.
41. Luyben, W.L., *Effect of solvent on controllability in extractive distillation.* Industrial & engineering chemistry research, 2008. **47**(13): p. 4425-4439.
42. WANG, Y., Q. LI, R. LI, J. QI, L. ZHANG, X. SONG, and C. PENG, *Simulation of the separation of acetone-methanol systems by positive and reverse extractive distillation.* Journal of Beijing University of Chemical Technology, 2020. **47**(1): p. 20.
43. Yang, S., Y. Wang, G. Bai, and Y. Zhu, *Design and control of an extractive distillation system for benzene/acetonitrile separation using dimethyl sulfoxide as an entrainer.* Industrial & Engineering Chemistry Research, 2013. **52**(36): p. 13102-13112.
44. Díaz, C. and J. Tojo, *Phase equilibria behaviour of n-heptane with o-xylene, m-xylene, p-xylene and ethylbenzene at 101.3 kPa.* The Journal of Chemical

doi:10.6342/NTU202301003

Thermodynamics, 2002. **34**(12): p. 1975-1984.
45. Liu, K., T. Zhang, Y. Ma, J. Gao, D. Xu, L. Zhang, and Y. Wang, *Vapour-liquid equilibrium measurements and correlation for separating azeotropic mixture (ethyl acetate+ n-heptane) by extractive distillation.* The Journal of Chemical Thermodynamics, 2020. **144**: p. 106075.
46. Hosgor, E., T. Kucuk, I.N. Oksal, and D.B. Kaymak, *Design and control of distillation processes for methanol–chloroform separation.* Computers & chemical engineering, 2014. **67**: p. 166-177.
47. Cao, Y., J. Hu, H. Jia, G. Bu, Z. Zhu, and Y. Wang, *Comparison of pressure-swing distillation and extractive distillation with varied-diameter column in economics and dynamic control.* Journal of Process control, 2017. **49**: p. 9-25.
48. Ravagnani, M., M. Reis, R. Maciel Filho, and M. Wolf-Maciel, *Anhydrous ethanol production by extractive distillation: A solvent case study.* Process Safety and Environmental Protection, 2010. **88**(1): p. 67-73.
49. Gil, I., L. García, and G. Rodríguez, *Simulation of ethanol extractive distillation with mixed glycols as separating agent.* Brazilian Journal of Chemical Engineering, 2014. **31**: p. 259-270.
50. Jaime, J.s.A., G. Rodríguez, and I.n.D. Gil, *Control of an optimal extractive distillation process with mixed-solvents as separating agent.* Industrial & Engineering Chemistry Research, 2018. **57**(29): p. 9615-9626.
51. Yang, X.-L. and J.D. Ward, *Extractive distillation optimization using simulated annealing and a process simulation automation server.* Industrial & Engineering Chemistry Research, 2018. **57**(32): p. 11050-11060.
52. Douglas, J.M., *Conceptual design of chemical processes*. 1988: McGraw-Hill New York.
53. Turton, R., R.C. Bailie, W.B. Whiting, and J.A. Shaeiwitz, *Analysis, synthesis and design of chemical processes*. 2008: Pearson Education New Jersey.
54. Laroche, L., N. Bekiaris, H.W. Andersen, and M. Morari, *The curious behavior of homogeneous azeotropic distillation—implications for entrainer selection.* AIChE Journal, 1992. **38**(9): p. 1309-1328.
55. Wang, Q., B. Yu, and C. Xu, *Design and control of distillation system for methylal/methanol separation. Part 1: extractive distillation using DMF as an entrainer.* Industrial & engineering chemistry research, 2012. **51**(3): p. 1281-1292.
56. Wu, Y.C., P.H.-C. Hsu, and I.-L. Chien, *Critical assessment of the energy-saving potential of an extractive dividing-wall column.* Industrial & Engineering Chemistry Research, 2013. **52**(15): p. 5384-5399.
57. Cordeiro, G.n.M., M.F. de Figueirêdo, W.B. Ramos, F.c.A. Sales, K.D. Brito, and R.P. Brito, *Systematic strategy for obtaining a dividing-wall column applied to an*

doi:10.6342/NTU202301003

extractive distillation process. Industrial & Engineering Chemistry Research, 2017. **56**(14): p. 4083-4094.

58. Luyben, W.L., *Principles and case studies of simultaneous design*. 2012: John Wiley & Sons New Jersey.
59. Seider, W.D., J. Seader, D.R. Lewin, and S. Widagdo, *Product and process design principles: synthesis*. 2004: Wiley New Jersey.

doi:10.6342/NTU202301003

Appendix A. Optimization Variables

The optimization variables for each sequence are shown on process flow diagrams in Figure A-1 and are listed in Table A-1. The meaning of each optimization variable is given in Table A-2. Numbers 1, 2 and 3 in variables (e.g. NS1, FS2, etc.) refer to the column number. In sequences DCSSS and SDCSSS, the side-stream flowrate is not an optimization variable because it is manipulated to achieve the desired entrainer purity at the bottom of the extractive column (using the feature Design Spec feature in Aspen Plus).

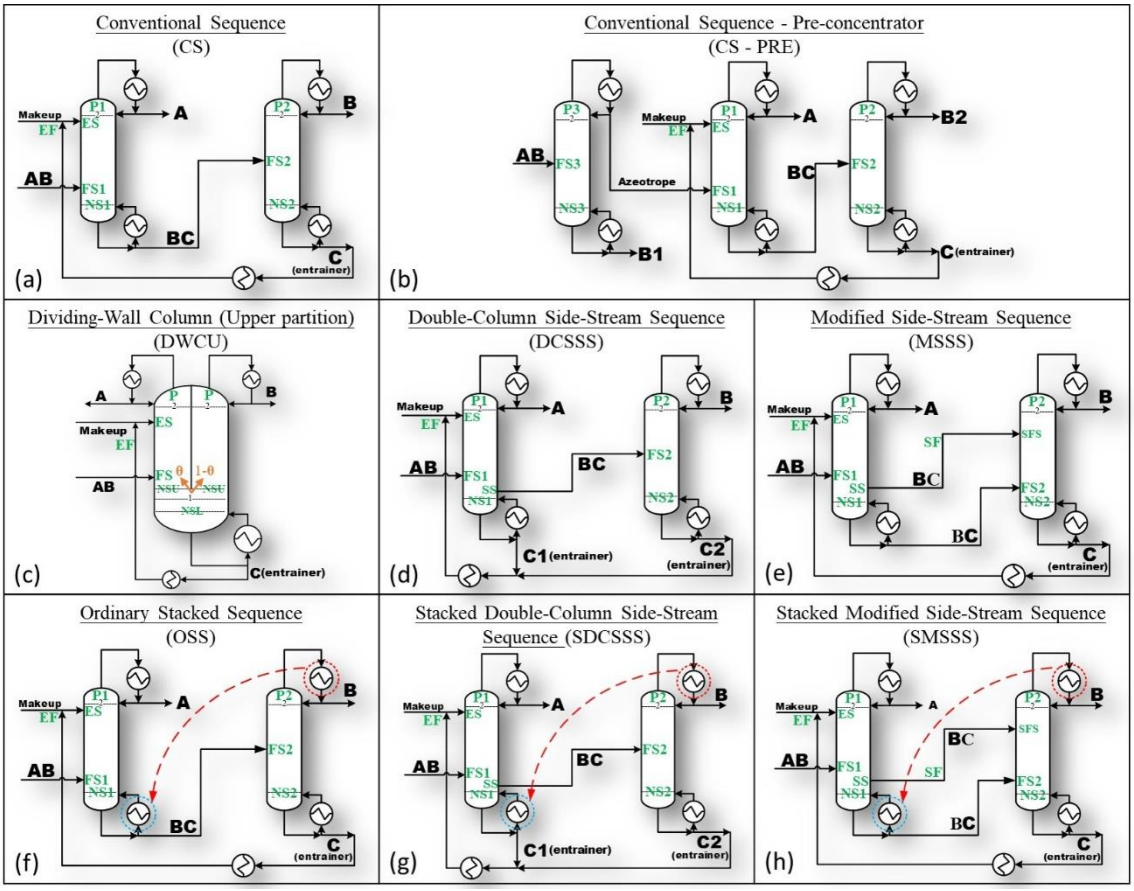

Figure A-1. Sequences labeled with optimization variables

doi:10.6342/NTU202301003

Table A-1. The optimization variables for each sequence

Sequence	Optimization variables
CS	NS1, FS1, P1, NS2, FS2, P2, ES, EF
CS-PRE	NS1, FS1, P1, NS2, FS2, P2, ES, EF, NS3, FS3, P3
DWCU	NSU, NSL, FS, ES, P, θ, EF
DCSSSS	NS1, FS1, SS, P1, NS2, SFS, P2, ES, EF
MSSS	NS1, FS1, SS, P1, NS2, FS2, SFS, P2, SF, ES, EF
OSS	NS1, FS1, P1, NS2, FS2, P2, ES, EF
SDCSSS	NS1, FS1, SS, P1, NS2, SFS, P2, ES, EF
SMSSS	NS1, FS1, SS, P1, NS2, FS2, SFS, P2, SF, ES, EF

Table A-2. Meaning of optimization variables labeled in Figure A-1

variable	meaning
NS	number of stages
ES	entrainer feed stage
FS	feed stage
SS	side stream withdraw stage
SFS	side stream feed stage
P	pressure
SF	side stream flowrate
EF	entrainer flowrate
NSU	number of stages of the upper section of DWCU
NSL	number of stages of the low section of DWCU
θ	vapor split ratio

doi:10.6342/NTU202301003

Appendix B. Binary Interaction Parameters

Table B-1. Binary interaction parameters for each case

Case No.	Model	Component i	Component j	Aij	Aji	Bij	Bji	Cij
1	NRTL	A	B	0	0	371.0837	446.8746	0.3
		A	C	0	0	422.264432	165.055855	0.3
		B	C	0	0	-472.685429	743.671394	0.3
2	NRTL	A	B	0	0	371.0837	446.8746	0.3
		A	C	0	0	354.057657	187.54339	0.3
		B	C	0	0	-447.326056	696.596957	0.3
3	NRTL	A	C	0	0	520.4172	-81.3518	0.3
		C	B	3.9884	-2.9678	-1165.8684	934.0338	0.3
		A	B	-1.7369	-0.899	903.214	442.4486	0.3
4	NRTL	B	C	0	0	-85.2188	128.5015	0.3
		A	B	1.89221	-0.711609	-0.0431461	6.33667	0.1
		A	C	-1.50415	-0.396552	758.949	136.021	0.5
5	UNIQUAC	A	B	0	0	39.0511	-280.377	0
		A	C	0	0	107.496708	-218.565883	0
		B	C	0	0	-47.6702671	12.8075994	0
6	NRTL	A	B	0	0	419.8083	40.004	0.3
		A	C	0	0	248.157164	307.945164	0.3
		B	C	0	0	-328.921683	592.477808	0.3
7	NRTL	C	B	0	0	-225.0495	315.849	0.3
		A	B	0.783184	0.907431	0	0	0.5
		A	C	4.07242	0.196083	-1244.66	341.63	0.5
8	NRTL	A	B	-0.156	1.6271	459.8772	214.0758	0.45
		A	C	9.62547	-5.70134	-2370.19	1427.36	0.104156
		B	C	-2.40877	1.37311	959.52	-478.48	0.3
9	NRTL	A	C	0	0	520.4172	-81.3518	0.3
		C	B	3.9884	-2.9678	-1165.8684	934.0338	0.3
		A	B	-1.7369	-0.899	903.214	442.4486	0.3
10	UNIQUAC	A	B	0	0	-225.1533	52.7705	0
		A	C	8.6051	-4.8338	-3122.5818	1612.1963	0
		B	C	-1.0662	0.6437	432.8785	-322.1312	0
11	WILSON	A	B	0	0	-154.103	-217.9322	0
		A	C	0	0	-138.4803	-370.594	0
		B	C	0	0	111.452764	-111.016394	0
12	NRTL	A	B	0	0	419.8083	40.004	0.3
		A	C	0	0	248.157164	307.945164	0.3
		B	C	0	0	-328.921683	592.477808	0.3
13	UNIQUAC	A	B	0	0	-225.1533	52.7705	0
		A	C	8.6051	-4.8338	-3122.5818	1612.1963	0
		B	C	-1.0662	0.6437	432.8785	-322.1312	0
14	WILSON	A	B	1.00741	1.03185	-485.608	-586.376	0
		A	C	-1.0367	0.1258	375.8305	-225.4925	0
		B	C	0.7975	-0.3312	-414.0103	140.9931	0
15	NRTL	A	B	-2.28748	1.3212	1431.82	-471.749	0.322401
		A	C	-3.06839	0.661605	1635.33	-385.763	0.318373
		B	C	1.2971	-1.48426	-386.394	451.806	0.5
16	NRTL	A	B	-0.8009	3.4578	246.18	-586.0809	0.3
		A	C	14.8422	-0.1115	-4664.4058	157.5937	0.47
		B	C	0.3479	-0.0567	34.8234	-147.1373	0.3
17	NRTL	A	B	-0.8009	3.4578	246.18	-586.0809	0.3
		A	C1	14.8422	-0.1115	-4664.4058	157.5937	0.47
		B	C1	0.3479	-0.0567	34.8234	-147.1373	0.3
		A	C2	0	0	442.713	36.139	0.3
		B	C2	-1.2515	-0.7318	272.6075	170.9167	0.3
		C1	C2	0	0	298.1435	-347.5824	0.3

Table B-1 shows the binary interaction parameters for each chemical system.

doi:10.6342/NTU202301003

Appendix C. Parameters for SA Algorithm

Figure C-1 shows how the parameters for SA are determined, including initial temperature (T_0), finial temperature (T_f), decrement rate (R), and iteration time (N_i).

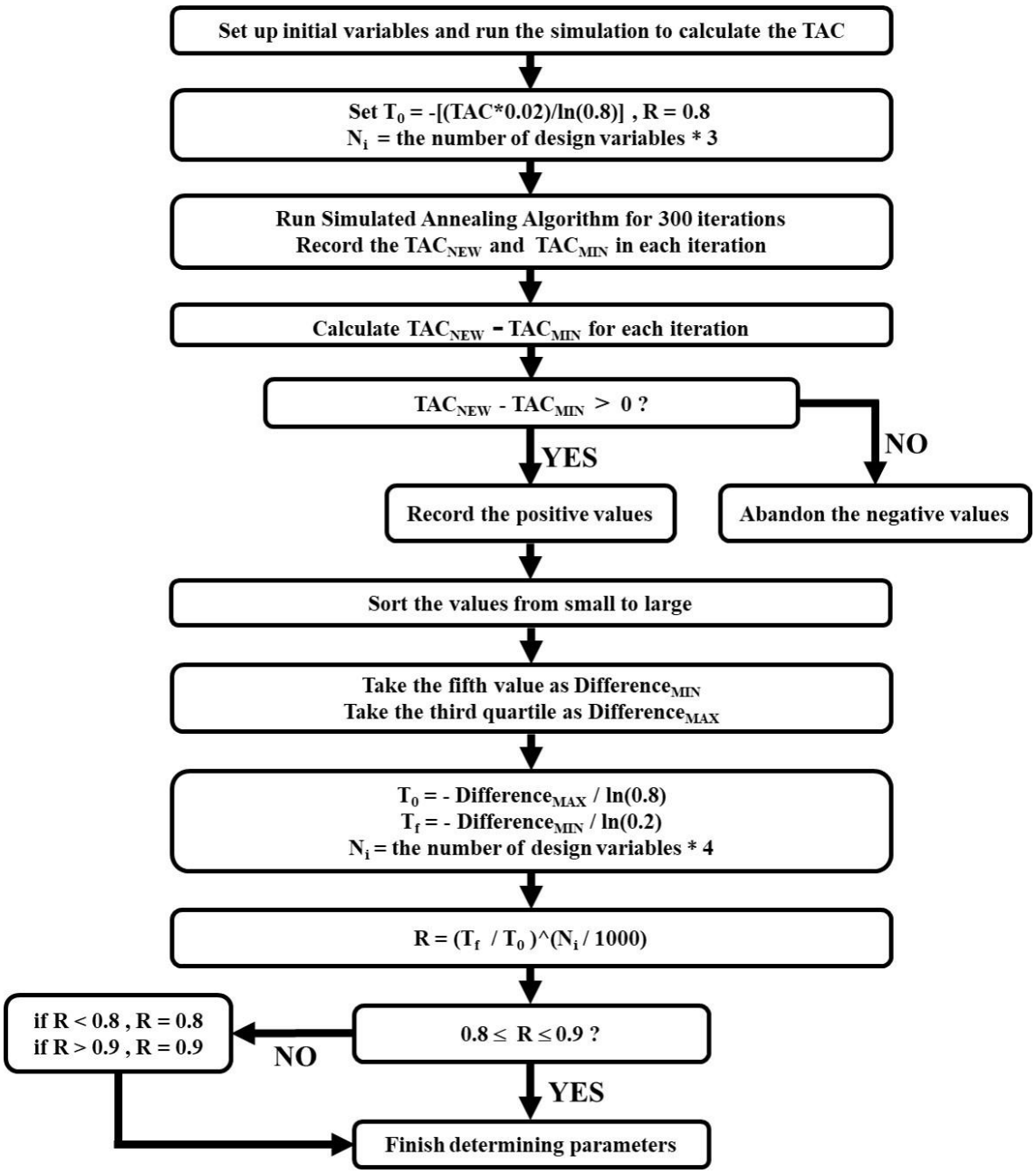

Figure C-1. The flowchart for calculating parameters for the simulated annealing (SA) algorithm

doi:10.6342/NTU202301003

Appendix D. Economic Evaluation

Methods and equations for cost calculations are presented in this section This material is based on the work of Douglas[52], Luyben [58], Seider et al. [59], and Turton et al [53].

1. Column Capital Cost

$$\text{Column Capital Cost} = 3015 \times (2.18 + 3.67 \times F_p) \times CD^{1.066} \times H^{0.802}$$

CD[m] = column diameter

H[m] = column height = $0.73152 \times (NS - 1)$

NS = number of stages

F_p = pressure factor

Pressure (atm) ≤	3.4	6.9	13.8	20.5
F_P	1	1.05	1.15	1.2

For DWCU:

CD = sqrt(max([CD1^2+CD3^2, CD4^2])) = Shell diameter

CD1 = pre-fractionator column diameter

CD3 = side column diameter

CD4 = stripping column diameter

2. Reboiler Cost

$$\text{Reboiler Capital Cost} = 7296 \times A_R^{0.65}$$

$A_R[m^2]$ = heat transfer area = $\frac{Q_R}{U_R \times \triangle T_R}$

Q_R (kW) = reboiler duty

U_R (kW/m^{2}K) = heat transfer coefficient = 0.568

$\triangle T_R = T_{steam} - T_{reboiler}$

The minimum temperature difference is set to be 10 ˚C.

Table D-1. Prices of hot utilities

Steam	Pressure	Temperature	Price ($/GJ)
High pressure stream	42 bar	254°C	9.88
Middle pressure stream	11 bar	184°C	8.22
Low pressure stream	6 bar	160°C	7.78

a. $T_{reboiler} < 150$ ˚C.

$$\text{Operating Cost } \left[\frac{\text{USD}}{8000\text{hr}}\right] = 7.78*RD/10\text{^}6*3600*8000$$

Temperature of low pressure stream = 160 ˚C.

doi:10.6342/NTU202301003

b. $T_{\text{reboiler}} < 174^{\circ}\text{C}$.

$$\text{Operating Cost } \left[\frac{\text{USD}}{8000\text{hr}}\right] = 8.22*\text{RD}/10\text{^}6*3600*8000$$

Temperature of middle pressure stream = 184°C

c. $T_{\text{reboiler}} < 244^{\circ}\text{C}$.

$$\text{Operating Cost } \left[\frac{\text{USD}}{8000\text{hr}}\right] = 9.88*\text{RD}/10\text{^}6*3600*8000$$

Temperature of high pressure stream = 254°C

3. Condenser Cost

$$\text{Condenser Capital Cost} = 7296 \times A_{\text{C}}^{0.65}$$

A_C [m^2] = heat transfer area = $\frac{Q_C}{U_C \times \triangle T_C}$

Q_C (kW) = condenser duty

U_C (kW/m^2K) = heat transfer coefficient = 0.852

ΔT_c = temperature difference between condenser and coolant

The minimum temperature difference is set to be 10°C.

Table D-2. Prices of cold utilities

Coolant	Temperature	Price ($/GJ)
Cooling water	41.85°C	0.354
Chilled water	5°C	4.43
Refrigerant	−20°C	7.89
Refrigerant	−50°C	13.11

a. $T_{\text{condenser}} > 51.85℃$

$\Delta T_C = T_{\text{condenser}} - 41.85$

$$\text{Operating Cost } \left[\frac{\text{USD}}{8000\text{hr}}\right] = 0.354 * (-ConD)/10\text{^}6 * 3600 * 8000$$

Temperature of cooling water = 41.85℃

b. $T_{\text{condenser}} > 25℃$

$\Delta T_C = 10/\ ln((T_{\text{condenser}} - 5)/(T_{\text{condenser}} - 15))$

$$\text{Operating Cost } \left[\frac{\text{USD}}{8000\text{hr}}\right] = 4.43 * (-\text{ConD})/10\text{^}6 * 3600 * 8000$$

Temperature of chilled water = 5℃, returned at 15℃

c. $T_{\text{condenser}} > -10℃$

$\Delta T_C = T_{\text{condenser}} + 20$

$$\text{Operating Cost } \left[\frac{\text{USD}}{8000\text{hr}}\right] = 7.89 * (-\text{ConD})/10\text{^}6 * 3600 * 8000$$

Temperature of refrigerant = −20℃

doi:10.6342/NTU202301003

d. $T_{\text{condenser}} > -50℃$

$\Delta T_C = T_{\text{condenser}} + 50$

$$\text{Operating Cost}\left[\frac{\text{USD}}{8000\text{hr}}\right] = 13.11 * (-\text{ConD1})/10\text{^}6 * 3600 * 8000$$

Temperature of refrigerant = −50℃

4. Heat Exchanger Cost

$$\text{Heat exchanger Capital Cost} = 7296 \times A_{HX}^{0.65}$$

$A_{HX}[m^2]$ = heat transfer area = $\frac{Q_{HX}}{U_{HX} \times \triangle T_{HX}}$

Q_R (kW) = heat exchanger duty

U_{HX} (kW/m^{2}K) = heat transfer coefficient = 0.852

$\triangle T_{HX} = T_{hot} - T_{cold}$

5. Vacuum Cost

Two types of vacuum systems are considered when the column pressure is lower than atmosphere, and the one with the lower TAC would be selected.

5.1. Steam-Jet Ejector

$$\text{Steam cost of the ejector} = 10 \times M_S \times S_{LP} \times 8000$$

$M_S \left[\frac{lb}{hr}\right]$ = mass flowrate of outlet vapor from precondenser

$S_{LP} \left[\frac{\$}{hr}\right]$ = low pressure stream cost = 0.004

S = size factor = $\frac{M_S}{P \times 760}$

P [atm] = Column Pressure

a. $P > \frac{100}{760}$ (One-stage)

$$\text{Capital cost of the ejector} = 0.1^{0.41} \times \frac{21665700}{M_S}$$

b. $\frac{2}{760} \leq P \leq \frac{100}{760}$ (Two-stage)

$$\text{Capital cost of the ejector} = 1.8 \times S^{0.41} \times \frac{21665700}{M_S}$$

c. $P < \frac{2}{760}$ (Three-stage)

doi:10.6342/NTU202301003

$$\text{Capital cost of the ejector} = 2.1 \times S^{0.41} \times \frac{21665700}{M_S} \times [ceil(\frac{S}{100})]^{1.59}$$

5.2. Liquid-Ring Pumps

$$\text{Operating cost of the pump} = 0.04 \times NW \times 8000$$

$V_S\ [\frac{ft^3}{min}]$ = volume flow rate of vapor from precondenser

NW [kW] = compressor power

P [atm] = column Pressure

a. $V_s < 50$

$$\text{Capital cost of the pump} = 50^{0.35} \times \frac{10588500}{M_S}$$

b. $50 \leq V_s \leq 350$

$$\text{Capital cost of the pump} = V_S{}^{0.35} \times \frac{10588500}{M_S}$$

c. $V_s > 350$

$$\text{Capital cost of the pump} = V_S{}^{0.41} \times \frac{10588500}{M_S} \times [\text{ceil}(\frac{V_S}{100})]^{1.65}$$

6. Liquid Pump Cost

$$\text{Capital cost} = 10^{(3.3892+0.0536\times\log_{10}(PP)+0.1538\times\log_{10}(PP)^2)}$$

$$\text{Electricity cost} = 0.0674 \times PP \times 8000$$

PP [KW] = power of the pump

doi:10.6342/NTU202301003

Example of cost and energy consumption calculations

An example of how TAC and energy consumption Q are calculated is given below. Taking the ordinary stacked sequence (OSS) of Case No.5 for instance, Table D-3 shows the required information for calculating TAC. The word "original" refers to the raw data from Aspen Plus, and the word "real" means the real duty of the condenser and the reboiler after stacking. For non-stacked sequences, the real duty equals the original duty, whereas for stacked sequences, the calculation of the real duty follows the formula below. If the original reboiler duty is larger than the original condenser duty:

$$\text{Real Reboiler Duty} = \text{Orginal Reboiler Duty} - |\text{Original Condenser Duty}|$$

$$\text{Real Condenser Duty} = 0$$

$$\text{Heat Exchanger Duty} = |\text{Original Condenser Duty}|$$

If the original reboiler duty is smaller than the original condenser duty:

$$\text{Real Reboiler Duty} = 0$$

$$\text{Real Condenser Duty} = |\text{Orginal Condenser Duty}| - \text{Original reboielr Duty}$$

$$\text{Heat Exchanger Duty} = \text{Original Reboiler Duty}$$

Table D-3. The required information for calculating TAC (Ordinary Stacked Sequence, Case No.5)

Variables	Extractive Column	Recovery Column
Number of Stages	36	23
Column Diameter (m)	1.07	0.95
Column Pressure (atm)	1	2.3
Original Condenser Duty (kW)	-741	-877
Real Condenser Duty (kW)	-741	0
Original Reboiler Duty (kW)	1197	1155
Real Reboiler Duty (kW)	319	1155
Condenser Temperature (°C)	56	129.3
Reboiler Temperature (°C)	118	179.9
Cooler Duty (kW)	-497	
Heat Exchanger Duty (kW)	877	

Energy consumption Q is the total reboiler duty, which is 319 plus 1155 kW. The column capital cost is:

$$\text{Column Capital Cost} = 3015 \times (2.18 + 3.67 \times F_p) \times CD^{1.066} \times 0.73152 \times (NS - 1)^{0.802}$$

As the pressure is lower than 3.4 atm, the pressure factor F_p remains to be one. The column cost will be:

$$\text{The 1st column} = 3015 \times (2.18 + 3.67 \times 1) \times 1.07^{1.066} \times 0.73152 \times (36 - 1)^{0.802}$$

$$\text{The 2nd column} = 3015 \times (2.18 + 3.67 \times 1) \times 0.95^{1.066} \times 0.73152 \times (23 - 1)^{0.802}$$

doi:10.6342/NTU202301003

The capital cost of the reboiler, condenser, cooler, and heat exchanger is:

$$\text{Reboiler Cost (1st)} = 7296 \times \left(\frac{Q_{\text{R}}}{U_{\text{R}} \times \triangle T_{\text{R}}}\right)^{0.65} = 7296 \times \left(\frac{319}{0.568 \times (160 - 118)}\right)^{0.65}$$

$$\text{Reboiler Cost (2nd)} = 7296 \times \left(\frac{Q_{\text{R}}}{U_{\text{R}} \times \triangle T_{\text{R}}}\right)^{0.65} = 7296 \times \left(\frac{1155}{0.568 \times (254 - 179.9)}\right)^{0.65}$$

$$\text{Condenser Cost (1st)} = 7296 \times \left(\frac{Q_{\text{C}}}{U_{\text{C}} \times \triangle T_{\text{C}}}\right)^{0.65} = 7296 \times \left(\frac{741}{0.852 \times (56 - 41.85)}\right)^{0.65}$$

$$\text{Cooler Cost} = 7296 \times \left(\frac{Q_{\text{C}}}{U_{\text{C}} \times \text{LMTD}}\right)^{0.65} = 7296 \times \left(\frac{497}{0.852 \times \left(\frac{(179.9 - 5) - (50 - 5)}{\ln\left(\frac{179.9 - 5}{50 - 5}\right)}\right)}\right)^{0.65}$$

$$\text{Exchanger Cost} = 7296 \left(\frac{Q_{\text{HX}}}{U_{\text{HX}} \times \triangle T_{\text{HX}}}\right)^{0.65} = 7296 \times \left(\frac{877}{0.852 \times (129.3 - 118)}\right)^{0.65}$$

where Q_R is the reboiler duty (kW), Q_C is the condenser duty (kW), U_R is the heat transfer coefficient (kW/m^{2}k) for reboilers, U_C is the heat transfer coefficient (kW/m^{2}k) for condensers, $\triangle T_R$ is the temperature difference between the reboiler and the steam, $\triangle T_C$ is the temperature difference between the cold utilities and the condenser, and $\triangle T_{HX}$ is the temperature difference between the 2nd condenser and the 1st reboiler. The operating cost of the reboiler, condenser, and cooler is:

$$\textit{Reboiler Operating Cost}\ (1st) = 7.78\ (\$/GJ) \times \frac{319 \times 3600}{10^6}\ (GJ/hr) \times 8000\ (hr)$$

$$\textit{Reboiler Operating Cost}\ (2nd) = 9.88\ (\$/GJ) \times \frac{1155 \times 3600}{10^6}\ (GJ/hr) \times 8000\ (hr)$$

$$\textit{Condenser Operating Cost}\ (1st) = 0.354\ (\$/GJ) \times \frac{741 \times 3600}{10^6}\ (GJ/hr) \times 8000\ (hr)$$

$$\textit{Cooler Operating Cost}\ (1st) = 4.43\ (\$/GJ) \times \frac{497 \times 3600}{10^6}\ (GJ/hr) \times 8000\ (hr)$$

With these costs determined, TAC can be caluclated through the formula:

$$\text{TAC} = \text{Operating Cost (OC)} + \frac{\text{Capital Cost (CC)}}{3\ (\text{Payback Period})}$$

doi:10.6342/NTU202301003

Appendix E. TAC and Reboiler Duty of Each Sequence

Table E-1 shows the TAC and reboiler duty in absolute and percentage terms for sequences without stacking. The pre-concentrator sequence CS-PRE is considered only when the feed is far from the azeotropic composition. Table E-2 shows the TAC and reboiler duty in absolute and percentage terms for sequences with stacking.

doi:10.6342/NTU202301003

Table E-1. The TAC and reboiler duty of the non-stacked sequences for each case

Case No.	R_{CB}		Total Annual Cost (TAC*10^3)						Reboiler Duty Q(kW)				
			CS	MSSS	DCSSS	DWCU	CS-PRE		CS	MSSS	DCSSS	DWCU	CS-PRE
1	0.17	TAC%	100%	99.7%	107.5%	108.1%	148.0%	Q%	100%	94.1%	96.2%	97.6%	142.4%
		TAC	$514	$512	$552	$555	$760	Q	1399	1317	1345	1366	1992
2	0.18	TAC%	100%	99.2%	101.3%	102.9%	128.1%	Q%	100%	94.0%	94.8%	101.5%	123.4%
		TAC	$572	$568	$580	$589	$733	Q	1558	1464	1477	1581	1923
3	0.44	TAC%	100%	99.1%	102.0%	105.6%	108.5%	Q%	100%	96.6%	97.5%	100.7%	105.8%
		TAC	$873	$865	$891	$922	$947	Q	2350	2269	2290	2366	2486
4	0.86	TAC%	100%	97.1%	98.9%	100.8%	149.6%	Q%	100%	96.0%	95.3%	97.0%	149.6%
		TAC	$774	$752	$766	$781	$1,159	Q	2173	2086	2070	2108	3251
5	0.88	TAC%	100%	98.9%	102.2%	103.8%	133.0%	Q%	100%	96.7%	96.5%	99.1%	135.3%
		TAC	$734	$727	$751	$762	$977	Q	2,033	1966	1962	2016	2654
6	1.59	TAC%	100%	97.0%	99.0%	101.3%	127.2%	Q%	100%	94.3%	94.4%	96.2%	125.6%
		TAC	$830	$805	$822	$840	$1,055	Q	2425	2286	2288	2333	3046
7	1.68	TAC%	100%	93.7%	95.0%	102.6%	-	Q%	100%	90.3%	93.0%	95.7%	-
		TAC	$1,158	$1,085	$1,100	$1,188	-	Q	3174	2866	2951	3039	-
8	2.21	TAC%	100%	95.4%	102.7%	113.0%	-	Q%	100%	91.6%	99.4%	112.5%	-
		TAC	$1,273	$1,215	$1,308	$1,439	-	Q	3193	2925	3175	3593	-
9	2.70	TAC%	100%	98.5%	99.1%	110.3%	-	Q%	100%	94.0%	94.4%	104.0%	-
		TAC	$891	$878	$883	$983	-	Q	2387	2244	2253	2483	-
10	3.10	TAC%	100%	97.2%	98.2%	102.1%	-	Q%	100%	94.9%	95.2%	97.2%	-
		TAC	$920	$894	$904	$940	-	Q	2600	2468	2476	2528	-
11	3.60	TAC%	100%	94.9%	103.4%	107.6%	-	Q%	100%	94.6%	96.4%	98.7%	-
		TAC	$982	$932	$1,015	$1,057	-	Q	2724	2577	2627	2690	-
12	4.60	TAC%	100%	95.8%	97.0%	99.0%	-	Q%	100%	91.5%	92.5%	93.1%	-
		TAC	$883	$847	$857	$875	-	Q	2587	2367	2393	2408	-
13	8.20	TAC%	100%	93.4%	94.0%	108.5%	-	Q%	100%	90.7%	92.2%	103.3%	-
		TAC	$1,047	$978	$984	$1,136	-	Q	2930	2656	2700	3025	-
14	9.30	TAC%	100%	86.4%	86.0%	88.0%	-	Q%	100%	84.3%	86.1%	87.8%	-
		TAC	$1,358	$1,174	$1,168	$1,195	-	Q	3692	3113	3177	3243	-
15	12.85	TAC%	100%	101.1%	74.0%	76.6%	-	Q%	100%	101.2%	69.5%	70.5%	-
		TAC	$3,318	$3,353	$2,454	$2,542	-	Q	10438	10565	7257	7356	-
16	5.2	TAC%	100.0%	100.6%	106.9%	108.0%	-	Q%	100.0%	99.5%	101.5%	102.5%	-
		TAC	$1,269	$1,277	$1,356	$1,371	-	Q	3711	3693	3768	3803	-
17	4.1	TAC%	100.0%	105.8%	112.2%	110.8%	-	Q%	100.0%	98.1%	102.5%	104.2%	-
		TAC	$1,239	$1,311	$1,391	$1,373	-	Q	3575	3507	3663	3726	-

doi:10.6342/NTU202301003

Table E-2. The TAC and reboiler duty of the stacked sequences

Case No.	R_{CB}		Total Annual Cost (TAC*10^3)					Reboiler duty Q(kW)			
			CS	OSS	SMSSS	SDCSSS		CS	OSS	SMSSS	SDCSSS
1	0.17	TAC%	100%	80.1%	81.2%	-	Q%	100%	64.9%	81.2%	-
		TAC	$514	$411	$417	-	Q	1399	908	923	-
2	0.18	TAC%	100%	75.9%	78.3%	86.2%	Q%	100%	57.6%	59.2%	64.8%
		TAC	$572	$434	$448	$493	Q	1558	897	923	1010
3	0.44	TAC%	100%	71.8%	71.6%	79.4%	Q%	100%	55.6%	55.1%	57.7%
		TAC	$873	$627	$626	$693	Q	2350	1306	1294	1357
4	0.86	TAC%	100%	81.7%	82.0%	89.8%	Q%	100%	68.2%	68.4%	71.1%
		TAC	$774	$633	$635	$695	Q	2173	1482	1486	1545
5	0.88	TAC%	100%	90.3%	92.2%	101.4%	Q%	100%	72.5%	73.9%	80.0%
		TAC	$734	$664	$677	$745	Q	2034	1474	1504	1627
6	1.59	TAC%	100%	83.9%	85.1%	90.2%	Q%	100%	67.9%	69.2%	73.1%
		TAC	$830	$696	$706	$749	Q	2425	1646	1678	1772
7	1.68	TAC%	100%	84.5%	85.7%	86.9%	Q%	100%	73.0%	73.2%	73.6%
		TAC	$1,158	$979	$992	$1,007	Q	3174	2317	2323	2335
9	2.70	TAC%	100%	92.0%	92.4%	91.8%	Q%	100%	83.8%	84.0%	82.6%
		TAC	$891	$820	$823	$818	Q	2387	2001	2005	1972
10	3.10	TAC%	100%	89.0%	-	80.4%	Q%	100%	76.5%	-	68.1%
		TAC	$4,020	$3,579[a]	-	$3,233 [a]	Q	13858	10600[a]	-	9440[a]
12	4.60	TAC%	100%	98.3%	98.6%	93.5%	Q%	100%	88.1%	88.2%	82.7%
		TAC	$883	$868	$871	$826	Q	2587	2279	2282	2140
13	8.20	TAC%	100%	96.4%	93.4%	89.1%	Q%	100%	65.5%	85.8%	81.6%
		TAC	$1,047	$1,009	$978	$933	Q	2930	1919	2515	2390
14	9.30	TAC%	100%	98.6%	99.3%	85.2%	Q%	100%	92.7%	93.3%	82.4%
		TAC	$1,358	$1,340	$1,349	$1,158	Q	3692	3422	3445	3043

[a] The TAC and the reboiler duty of OSS and SDCSSS for Case No. 10 are taken from Tututi et al. [21].

doi:10.6342/NTU202301003

Appendix F. Flowsheets for the 5th Interpretation

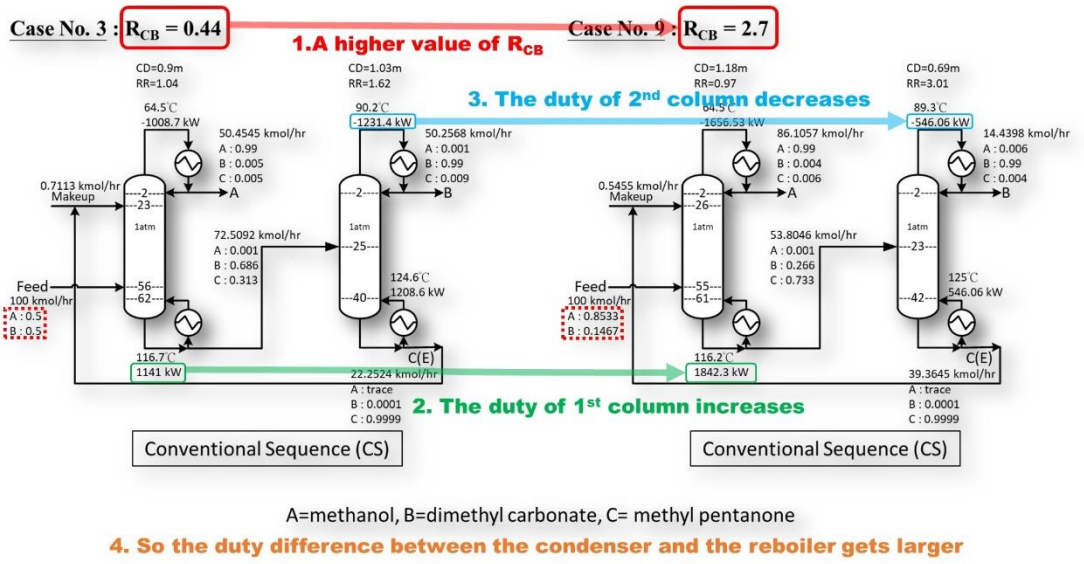

Figure F-1. The increase in duty difference between the 1st reboiler and the 2nd condenser caused by the decreased concentration of species B in the feed (Cases No.3 and No.9).

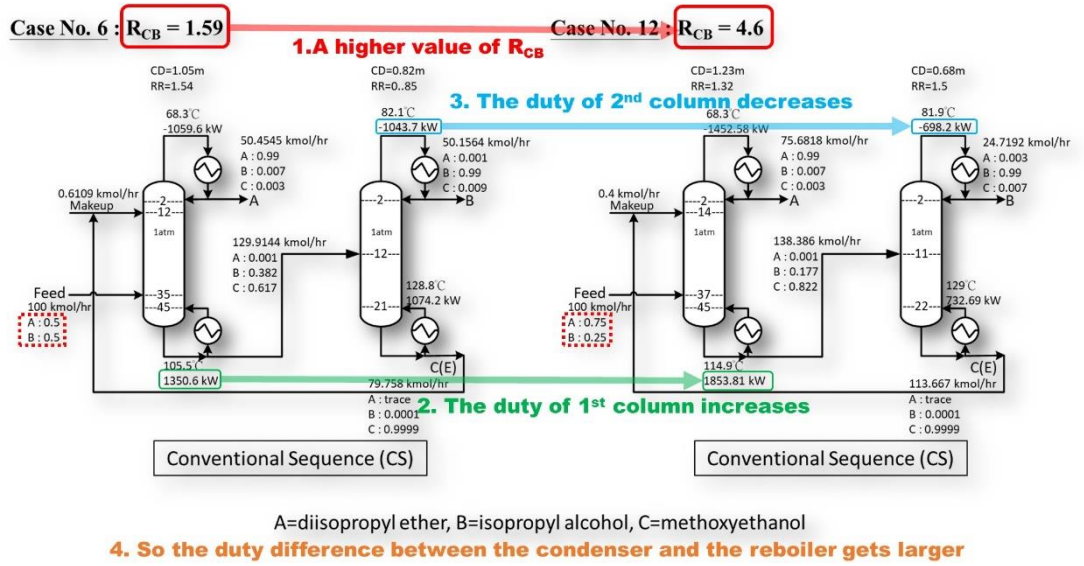

Figure F-2. The increase in duty difference between the 1st reboiler and the 2nd condenser caused by the decreased concentration of species B in the feed (Cases No.6 and No.12).

doi:10.6342/NTU202301003

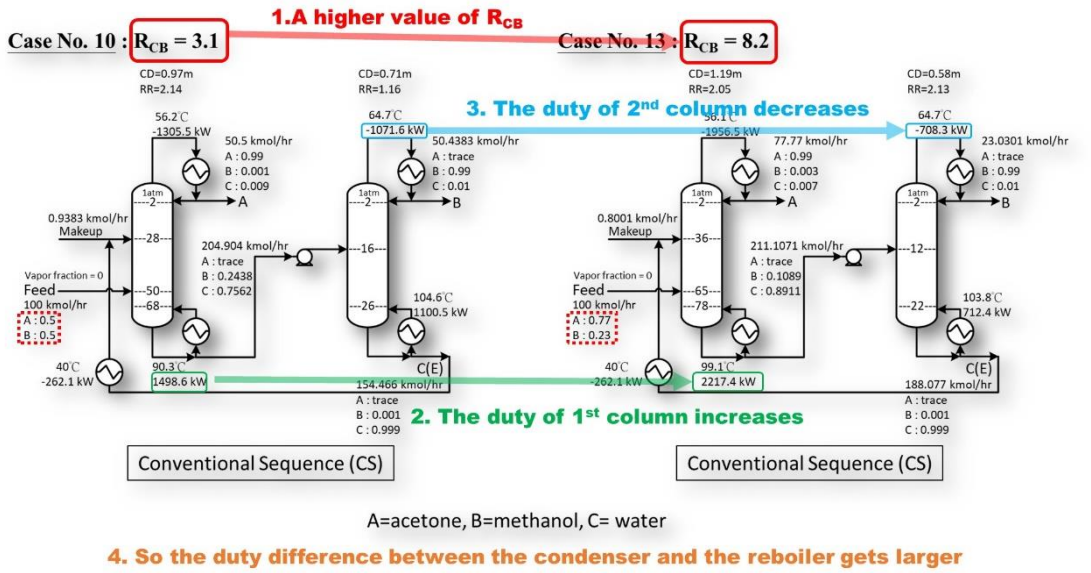

Figure F-3. The increase in duty difference between the 1st reboiler and the 2nd condenser caused by the decreased concentration of species B in the feed (Cases No.6 and No.12).

Figures F-1, F-2, and F-3 show three comparisons which illustrate the 5th interpretation of R_{CB}. An increased value of R_{CB} caused by the decreased concentration of B in the feed indicates that the feed is closer to the azeotropic composition, meaning that the extractive column separates a larger amount of the azeotropic mixture, so the duty of the 1st column increases. At the same time, the decreased concentration of B in the feed also indicates that the production rate of the heavy key in the recovery column is smaller, and a smaller amount of the heavy key needs to be vaporized from the feed of the recovery column, so the duty of the 2nd column decreases.

doi:10.6342/NTU202301003

Appendix G. The transition points of R_{CB}

Each trend line in this work is determined by fitting the data to a polynomial. The degree of the polynomial was determined by considering the tradeoff between accuracy and overfitting. In Figure 22, the polynomials are as follows:

$$\text{DCSSS TAC savings\%} = 0.0016R_{CB}^2 + 0.0007R_{CB} - 0.0163$$

$$\text{MSSS TAC savings\%} = -0.0003R_{CB}^3 + 0.004R_{CB}^2 - 0.002R_{CB} + 0.0165$$

The two curves cross at R_{CB}=8.4631≈8.4, so the boundary was taken to be 8.4. The data show some scatter. The values of the coefficient of determination (R^2) for the two curves are 0.867 and 0.659 for DCSSS and MSSS, respectively. The trend lines do generally describe the relative attractiveness of the two sequences. When R_{CB}<8.4, as the data shows, MSSS is better than DCSSS; when R_{CB}>8.4, DCSSS is better than MSSS. The curves in Figures 27 and 31 are determined the same way. In Figure 27, the polynomials are as follows:

$$\text{OSS TAC savings\%} = -0.00009R_{CB}^4 + 0.0013R_{CB}^3 - 0.00009R_{CB}^2 - 0.0615R_{CB} + 0.2381$$

$$\text{SDCSSS TAC savings\%} = 0.0002R_{CB}^4 - 0.0028R_{CB}^3 + 0.0161R_{CB}^2 - 0.045R_{CB} + 0.1659$$

$$\text{OSS-SDCSSS TAC savings\%} = -0.0008R_{CB}^3 + 0.0134R_{CB}^2 - 0.0876R_{CB} + 0.1385$$

The curve (OSS-SDCSSS) crosses the horizontal axis where the difference is zero at R_{CB}=2.2532≈2.2. In Figure 31, the polynomials are as follows:

$$\text{Stacking} = -0.0002R_{CB}^4 + 0.0028R_{CB}^3 - 0.0087R_{CB}^2 - 0.0454R_{CB} + 0.2457$$

doi:10.6342/NTU202301003

$$\text{Side streams} = 0.0107e^{0.2731R_{CB}}$$

$$\text{Stacking + Side Streams} = 0.0043R_{CB}^2 - 0.0476R_{CB} + 0.2159$$

The lower bound (where the trend line of stacking crosses the trend line of stacking + side streams) and the upper bound (where the trend line of side streams crosses the trend line of stacking + side streams) are 2.0619 and 10.7079, respectively. If the minimum contribution (TAC saving%) from side streams or stacking is set to be 1.3%, the lower bound and the upper bound become R_{CB}=2.6315≈2.6 and R_{CB}=8.4399≈8.4.

doi:10.6342/NTU202301003